

Rank-Learner: Orthogonal Ranking of Treatment Effects

Henri Arno¹ Dennis Frauen^{2,3} Emil Javurek^{2,3} Thomas Demeester¹ Stefan Feuerriegel^{2,3}

Abstract

Many decision-making problems require ranking individuals by their treatment effects rather than estimating the exact effect magnitudes. Examples include prioritizing patients for preventive care interventions, or ranking customers by the expected incremental impact of an advertisement. Surprisingly, while causal effect estimation has received substantial attention in the literature, the problem of directly learning *rankings of treatment effects* has largely remained unexplored. In this paper, we introduce *Rank-Learner*, a novel two-stage learner that directly learns the ranking of treatment effects from observational data. We first show that naïve approaches based on precise treatment effect estimation solve a harder problem than necessary for ranking, while our *Rank-Learner* optimizes a pairwise learning objective that recovers the true treatment effect ordering, without explicit CATE estimation. We further show that our *Rank-Learner* is Neyman-orthogonal and thus comes with strong theoretical guarantees, including robustness to estimation errors in the nuisance functions. In addition, our *Rank-Learner* is model-agnostic, and can be instantiated with arbitrary machine learning models (e.g., neural networks). We demonstrate the effectiveness of our method through extensive experiments where *Rank-Learner* consistently outperforms standard CATE estimators and non-orthogonal ranking methods. Overall, we provide practitioners with a new, orthogonal two-stage learner for ranking individuals by their treatment effects.

1. Introduction

Across many application domains, decision-makers must rank individuals by their treatment effects (Kamran et al., 2024). Such ranking problems arise especially when limited resources make it necessary to prioritize those who benefit most from the treatment.

Examples. In healthcare, clinicians need to triage patients according to who should receive intensive care during periods when demand exceeds capacity (Aquino et al., 2022; Vinay et al., 2021) or prioritize patients for preventive care (Kraus et al., 2024). In marketing, firms must decide which customers to target with retention offers or which prospects to reach with costly advertisements (Devriendt et al., 2021; Gharibshah & Zhu, 2021). In public policy, governments must decide which individuals to target with policy interventions (Card et al., 2018). In all of these settings, effective decision-making depends on the relative ordering of treatment effects rather than on their exact magnitudes.

Interestingly, the task of learning-to-rank individuals by their treatment effects from observational data has received relatively little attention (see Section 2), especially when compared to the extensive literature on estimating heterogeneous treatment effects. One reason is that standard learning-to-rank methods (Liu, 2011; Cao et al., 2007; Burges et al., 2005) are not directly applicable in this setting; such methods would require supervision via the relative ordering of treatment effects, but treatment effects are never directly observed in observational data (Rubin, 2005).

Instead, existing works aimed at ranking individuals by their treatment effects proceed *indirectly* by first estimating conditional average treatment effects (CATEs) from observational data (Künzel et al., 2019; Wager & Athey, 2018). Concretely, a naïve approach is to first estimate CATEs using state-of-the-art methods (e.g., two-stage learners such as the DR- and R-learners (Kennedy, 2023; Nie & Wager, 2021)) and then rank individuals according to their estimated effects. However, as we show later, this strategy solves a much harder learning problem than necessary for ranking. In contrast, only a few works have explored how to learn treatment effect rankings *directly* (Kamran et al., 2024; Vanderschueren et al., 2024), but none of these methods are Neyman-orthogonal and thus lack favorable theoretical properties (e.g., robustness to nuisance estimation error).

¹Ghent University - imec, Ghent ²LMU Munich, Munich

³Munich Center for Machine Learning (MCML). Correspondence to: Henri Arno <henri.arno@ugent.be>.

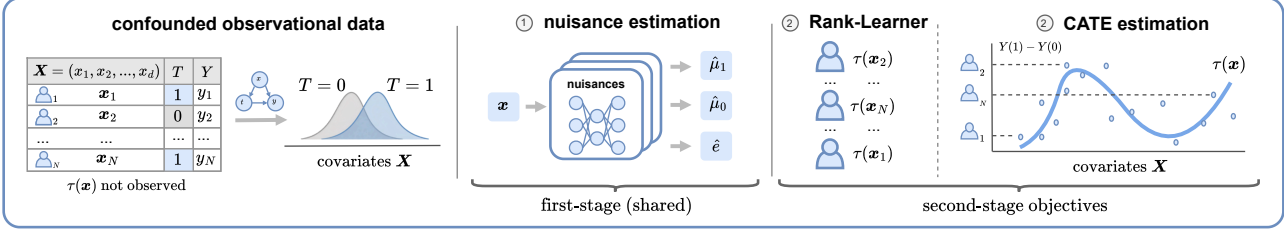


Figure 1. Two-stage learners for ranking treatment effects. *Left:* Confounded observational data with unobserved treatment effects. *Center:* First-stage estimation of nuisance functions (i.e., response surfaces and propensity score). *Right:* Second-stage objectives: our *Rank-Learner* vs. standard CATE estimation. Here, our proposed *Rank-Learner* directly optimizes a pairwise, Neyman-orthogonal ranking objective that targets the relative ordering of treatment effects. In contrast, standard CATE estimation optimizes a pointwise regression objective to recover treatment effect magnitudes, which is harder than necessary for ranking.

In this paper, we introduce ***Rank-Learner***, a novel two-stage learner for *ranking individuals by their treatment effects from observational data*. Rather than first estimating CATEs and then ranking individuals by their magnitudes, our *Rank-Learner* directly targets the ranking task itself by optimizing a population-level pairwise ranking objective, without explicit CATE estimation. This avoids solving the unnecessarily difficult problem of recovering precise treatment effects and instead focuses directly on the relevant quantity in our task, namely, the relative ordering of treatment effects between individuals (see Figure 1). Our *Rank-Learner* follows a two-stage approach: in the first stage, nuisance functions are estimated using flexible machine learning models; in the second stage, these estimates are plugged into a *novel orthogonal pairwise loss* to learn the ranking function. As a result, *Rank-Learner* is fully model-agnostic and can thus be instantiated with arbitrary machine learning models, such as neural networks. The orthogonality of our loss allows for favorable theoretical properties and ensures robustness to estimation errors in the nuisance functions. To the best of our knowledge, our *Rank-Learner* is the first orthogonal two-stage learner for ranking treatment effects.

Our main **contributions** are:¹ **(1)** We propose *Rank-Learner*, a novel two-stage learner for directly learning rankings of treatment effects from observational data. **(2)** We prove that the learning objective inside our *Rank-Learner* is Neyman-orthogonal. **(3)** We demonstrate that our *Rank-Learner* outperforms standard CATE estimators and non-orthogonal rankers across extensive experiments.

2. Related work

In this section, we review related work on (i) learning-to-rank, (ii) CATE estimation, and (iii) recent methods on ranking individuals by their treatment effects. An extended review on policy learning is given in Appendix A.

¹Code is available at <https://anonymous.4open.science/r/rank-learner>.

Learning-to-rank. Learning-to-rank refers to supervised learning methods for learning an ordering over a set of items (Liu, 2011). These approaches originate from information retrieval, where the goal is typically to rank documents for a given query based on relevance judgments. Existing methods can be classified into three broad categories depending on the type of supervision used during training: (i) *pointwise methods* define a loss using item-level relevance labels; (ii) *pairwise methods* rely on relevance comparisons between pairs of items and learn relative preferences (e.g., Burges et al., 2005); and (iii) *listwise methods* are supervised using entire ranked lists or permutations of items by relevance (e.g., Buyl et al., 2023; Cao et al., 2007). However, learning-to-rank methods are **not** directly applicable in our setting because the required supervision is unavailable since treatment effects are never directly observed.

CATE estimation. There is an extensive literature on estimating heterogeneous treatment effects from observational data, often formalized by the *conditional average treatment effect* (CATE). At a high level, existing approaches can be classified as *model-based* or *model-agnostic*. Model-based methods rely on specific machine learning models designed for treatment effect estimation, such as causal forests (Wager & Athey, 2018) or specialized neural networks (Shalit et al., 2017). Model-agnostic methods, also referred to as two-stage learners or meta-learners, define generic estimation procedures that can be instantiated with arbitrary machine learning models (Künzel et al., 2019).

State-of-the-art CATE estimators are *Neyman-orthogonal* two-stage learners, including the DR- and R-learners (Kennedy, 2023; Nie & Wager, 2021). In the first stage, so-called *nuisance functions* are estimated, which capture components of the data-generating process, like the treatment propensity and the conditional outcomes. In the second stage, treatment effects are estimated by optimizing a learning objective constructed from these nuisance estimates. Neyman-orthogonality ensures robustness of the second-stage model to estimation errors in the nuisance functions (Foster & Syrgkanis, 2023). However, the above methods

are designed to estimate the CATE *magnitudes*, but are **not** designed to directly learn a *ranking* of the CATEs.

Ranking of treatment effects. Recently, two works have explicitly considered the problem of ranking individuals by their treatment effects. Kamran et al. (2024) propose a tree-based method that directly optimizes a non-differentiable ranking criterion based on doubly robust pseudo outcomes (we refer to this method as *tree ranker*). In contrast, Vanderschueren et al. (2024) do not propose a new ranking method, but empirically evaluate different combinations of standard CATE estimators and conventional learning-to-rank objectives (our *plug-in ranker* baseline closely follows this strategy). However, **neither** approach is Neyman-orthogonal, implying that the resulting learning objectives are sensitive to estimation errors in the nuisance functions.

Research gap. Taken together, existing approaches either focus on estimating CATE magnitudes, or learn treatment-effect rankings using non-orthogonal learning objectives or model-specific classes. As summarized in Table 1, this leaves a gap for model-agnostic two-stage learners that directly target ranking, while remaining Neyman-orthogonal.

Method	Rank.	Agn.	Orth.	Reference
T-learner	✗	✓	✗	Künzel et al. (2019)
DR-learner	✗	✓	✓	Kennedy (2023)
Tree ranker	✓	✗	✗	Kamran et al. (2024)
Plug-in ranker	✓	✓	✗	cf. Vanderschueren et al. (2024)
Rank-learner (ours)	✓	✓	✓	<i>This work</i>

Table 1. Positioning of methods. *Rank.*: directly targets treatment effect ranking (rather than CATE magnitudes). *Agn.*: model-agnostic method that can be instantiated with arbitrary machine learning models. *Orth.*: Neyman-orthogonal learning objective with respect to nuisance estimation. T- and DR-learner are representative examples of two-stage learners for CATE estimation. Main experiments focus on two-stage learners, a comparison to *tree ranker* is given in Appendix F (Table 7).

3. Problem setup

Data. We consider a standard causal inference setting with observations $W = (X, T, Y) \sim \mathbb{P}$, where $X \in \mathcal{X} \subseteq \mathbb{R}^d$ represents covariates, $T \in \{0, 1\}$ is a binary treatment, and $Y \in \mathbb{R}$ is a continuous outcome. We assume that we have a dataset $\{x_i, t_i, y_i\}_{i=1}^n$ from $n \in \mathbb{N}$ individuals, sampled i.i.d. from \mathbb{P} . We build upon the potential outcomes framework (Rubin, 2005), meaning that each individual in the population has two potential outcomes, $Y(1)$ and $Y(0)$, where $Y(t)$ represents the outcome that we would observe had the treatment been $T = t$. Then, the CATE is defined as

$$\tau(x) = \mathbb{E}[Y(1) - Y(0) \mid X = x]. \quad (1)$$

Identification. Since potential outcomes are not directly observed, we rely on standard identification assumptions under which the CATE can be expressed in terms of the

observed data (Imbens & Rubin, 2015; Rosenbaum & Rubin, 1983).

Assumption 3.1 (Standard causal inference assumptions). For all $t \in \{0, 1\}$ and $x \in \mathcal{X}$, it holds: (i) *Consistency*: The observed outcome equals the potential outcome under the received treatment: $Y = Y(t)$ when $T = t$. (ii) *Positivity*: Each individual has a non-zero probability of receiving either treatment: $0 < e(x) < 1$ where $e(x) = P(T = 1 \mid X = x)$ is the propensity score. (iii) *Unconfoundedness*: There are no unmeasured confounders: $Y(t) \perp\!\!\!\perp T \mid X$.

Under Assumption 3.1, the CATE is identified as

$$\tau(x) = \mu_1(x) - \mu_0(x), \quad (2)$$

where $\mu_t(x) = \mathbb{E}[Y \mid T = t, X = x]$ are the conditional outcome regressions, referred to as *response surfaces*. Together with the propensity score $e(x)$, these response surfaces $\mu_1(x)$ and $\mu_0(x)$ constitute the *nuisance functions*, which we denote collectively as $\eta = (\mu_1, \mu_0, e)$.

Objective. In this work, we focus on ranking individuals by their treatment effects $\tau(x)$. To this end, we consider a real-valued *scoring function* $g : \mathcal{X} \rightarrow \mathbb{R}$, which is used to rank individuals based on their covariates. We require that the ordering of $g(x)$ agrees with that of $\tau(x)$, meaning that, for any $x, x' \in \mathcal{X}$, we have

$$g(x) > g(x') \quad \text{whenever} \quad \tau(x) > \tau(x'). \quad (3)$$

Equivalently, any scoring function of the form $g(x) = h(\tau(x))$, with h strictly increasing, induces the same ordering as $\tau(x)$. Throughout the paper, we assume that ties in $\tau(x)$ do not occur. Note that this task involves only ranking, and the magnitudes of $\tau(x)$ are *not* of direct interest.

4. Principles of orthogonal learning

Bias of plug-in rankers. A simple approach is to use *plug-in rankers*, which proceed by first estimating the nuisance functions $\hat{\mu}_t(x)$ (the response surfaces) from the observed data, and plugging these estimates into the identification formula from Eq. (2) to obtain $\hat{\tau}(x) = \hat{\mu}_1(x) - \hat{\mu}_0(x)$. These treatment effect estimates can then be used to construct the supervision targets for any learning-to-rank objective (examples discussed below), and g is fit by minimizing the corresponding empirical loss $\mathcal{L}^{\text{plug}}(g, \hat{\eta})$ (where $\hat{\eta}$ collects the estimated response surfaces). However, it is well established that such plug-in approaches suffer from *plug-in bias* (Kennedy, 2024): estimation errors in the nuisance functions enter the training objective directly, and spill over into the fitted scoring function g .

Neyman-orthogonality. Plug-in bias can be addressed by developing learning objectives that are *Neyman-orthogonal* with respect to the nuisance functions. Concretely, one first

estimates the nuisances $\hat{\eta}$ and then fits the target model by minimizing an objective $\mathcal{L}^{\text{corr}}(g, \hat{\eta})$ designed to be first-order insensitive to nuisance error. Formally, a loss is *orthogonal* if, for any perturbation directions Δg and $\Delta \eta$,

$$D_\eta D_g \mathcal{L}^{\text{corr}}(g^0, \eta^0)[\Delta g, \Delta \eta] = 0 \quad (4)$$

where D_η and D_g denote directional derivatives, η^0 are the true nuisance functions and g^0 is a population minimizer of $\mathcal{L}^{\text{corr}}(g, \eta^0)$ (Foster & Syrgkanis, 2023; Chernozhukov et al., 2018). Intuitively, this property means that the gradient of the loss with respect to g is robust against estimation errors in the nuisances. Orthogonality usually implies additional favorable properties, such as fast convergence rates (Foster & Syrgkanis, 2023; Nie & Wager, 2021).

Constructing orthogonal losses. A common strategy to obtain a Neyman-orthogonal objective is to start from the plug-in loss $\mathcal{L}^{\text{plug}}(g, \eta)$ and apply a correction based on its *influence function* (Kennedy, 2024; Foster & Syrgkanis, 2023). Intuitively, the influence function measures the first-order sensitivity of the population objective to infinitesimal perturbations of the data-generating distribution \mathbb{P} (for background and details, we refer to Appendix B). To the best of our knowledge, Neyman-orthogonal learning objectives for learning-to-rank treatment effects are currently missing.

5. Orthogonal ranking of treatment effects

Motivation. In this section, we first show that standard CATE learning solves a harder problem than required for ranking, and motivate a pairwise ranking objective instead. We then introduce a smooth surrogate loss that enables orthogonalization, and present our main contribution: a novel Neyman-orthogonal ranking loss that targets the treatment effect ordering directly. This learning objective forms the basis of our *Rank-Learner* (Section 6).

Why CATE learning is harder than needed for ranking. A naïve strategy to learn the treatment effect ordering is to first estimate CATEs and then rank individuals by these estimates. This corresponds to learning a scoring function g by minimizing the mean squared error loss

$$\mathcal{L}^{\text{cate}}(g, \eta) = \mathbb{E}_X \left[(g(X) - \tau(X))^2 \right], \quad (5)$$

which is the canonical population objective for standard CATE estimation (Morzywolek et al., 2024). The loss $\mathcal{L}^{\text{cate}}$ is uniquely minimized at $g(x) = \tau(x)$, and therefore requires recovering the *full* CATE function. While this, of course, gives the correct ranking, it is also unnecessarily difficult because we do not need correct treatment effect magnitudes. Below, we relax the optimization objective accordingly.

Why a ranking loss is preferred. Since ranking only depends on the *relative* ordering of treatment effects, we con-

sider the pairwise ranking objective (Burges et al., 2005)²

$$\mathcal{L}^{\text{bin}}(g, \eta) = \mathbb{E}_{X, X'} \left[\ell(p_g(X, X'), b_\tau(X, X')) \right], \quad (6)$$

where $\ell(p, t) = -t \log p - (1-t) \log(1-p)$ denotes the binary cross-entropy loss (we will use this shorthand notation throughout), and

$$p_g(X, X') = \sigma(g(X) - g(X')), \quad (7)$$

$$b_\tau(X, X') = \mathbf{I}\{\tau(X) > \tau(X')\}, \quad (8)$$

where $\sigma(\cdot)$ is the logistic sigmoid and $\mathbf{I}\{\cdot\}$ the indicator function. Here, $p_g(X, X')$ can be interpreted as a *pairwise preference probability* that encodes the model's confidence that X should be ranked ahead of X' . The label $b_\tau(X, X')$ provides the corresponding supervision by indicating whether X has a larger treatment effect than X' . Optimizing this loss yields a single scoring function g that can be used to rank individuals directly at inference.

At the population level, the infimum of \mathcal{L}^{bin} (which is not attainable by any finite g) can be approached arbitrarily closely by *any scoring function that preserves the treatment effect ordering*. In particular, any $g(x) = h(\tau(x))$ with h strictly increasing is population-optimal in this sense. This implies invariance to the form h , as long as it preserves the effect ordering. In contrast to $\mathcal{L}^{\text{cate}}$, which identifies treatment effect magnitudes, \mathcal{L}^{bin} imposes only ordering constraints on g . Since our goal is to recover only the ordering of treatment effects, we therefore focus on the *easier* loss \mathcal{L}^{bin} (see Appendix D for details).

Smooth surrogate ranking loss. So far, we have assumed oracle access to $\tau(x)$, but, in observational data, the treatment effect $\tau(x)$ is unobserved. Simply replacing $\tau(x)$ with an estimate $\hat{\tau}(x)$ suffers from plug-in bias, motivating an influence-function-based correction (cf. Section 4). However, to orthogonalize \mathcal{L}^{bin} via the influence function, the loss must depend smoothly on the treatment effects (and more generally, on the nuisance components η of the data-generating process). Since \mathcal{L}^{bin} uses the indicator targets $b_\tau(X, X')$ that are discontinuous, it is non-differentiable with respect to τ . To overcome this, we replace these binary targets with smooth probabilistic surrogates and consider the soft ranking loss (cf. Vandershueren et al., 2024)

$$\mathcal{L}^{\text{soft}}(g, \eta) = \mathbb{E}_{X, X'} \left[\ell(p_g(X, X'), t_\tau(X, X')) \right], \quad (9)$$

where

$$t_\tau(X, X') = \sigma \left(\frac{\tau(X) - \tau(X')}{\kappa} \right), \quad (10)$$

²Throughout, $\mathbb{E}_{X, X'}$ denotes the expectation over i.i.d. draws $X, X' \sim \mathbb{P}(X)$, and $\mathbb{E}_{W, W'}$ over $W, W' \sim \mathbb{P}$ analogously.

and $\kappa > 0$ is a smoothness parameter. These targets can be interpreted as the probability that X has a larger treatment effect than X' . The parameter κ controls how sharp this comparison is: smaller values push the targets closer to the binary indicators $b_\tau(X, X') \in \{0, 1\}$, larger values produce softer targets closer to 0.5. Crucially, this smoothness is what allows us to orthogonalize the ranking objective.

Our novel Neyman-orthogonal ranking loss. Since the targets in $\mathcal{L}^{\text{soft}}$ are smooth in τ , we can now orthogonalize this loss based on its influence function. Doing so introduces a correction that is expressed in terms of the full observational units $W = (X, T, Y)$, and leads to the following theorem.

Theorem 5.1 (Neyman-orthogonality). *We define the loss*

$$\mathcal{L}^{\text{orth}}(g, \eta) = \mathbb{E}_{W, W'} [\ell(p_g(X, X'), \tilde{t}_\eta(W, W'))], \quad (11)$$

with pseudo labels

$$\tilde{t}_\eta(W, W') = t_\tau(X, X') + \omega_\tau(X, X') \Delta_\eta(W, W'), \quad (12)$$

where

$$\omega_\tau(X, X') = \frac{1}{\kappa} t_\tau(X, X') (1 - t_\tau(X, X')), \quad (13)$$

$$\Delta_\eta(W, W') = (\phi_\eta(W) - \tau(X)) - (\phi_\eta(W') - \tau(X')), \quad (14)$$

with $\phi_\eta(W)$ the doubly robust score

$$\begin{aligned} \phi_\eta(W) = & \frac{T}{e(X)} (Y - \mu_1(X)) - \frac{1-T}{1-e(X)} (Y - \mu_0(X)) \\ & + \mu_1(X) - \mu_0(X). \end{aligned} \quad (15)$$

Then the loss $\mathcal{L}^{\text{orth}}(g, \eta)$ is Neyman-orthogonal with respect to the nuisance components $\eta = (\mu_1, \mu_0, e)$.

Proof. See Appendix C.

Theorem 5.1 shows that the proposed objective $\mathcal{L}^{\text{orth}}(g, \eta)$ is first-order insensitive to nuisance estimation error, but we need to verify that it still targets the correct treatment effect ordering. Therefore, we characterize its population minimizers evaluated at the true nuisance functions.

Theorem 5.2 (Minimizers of the orthogonal loss). *Let η^0 denote the true nuisance functions, and let τ^0 be the corresponding CATE. For any fixed and finite $\kappa > 0$, the orthogonal ranking loss $\mathcal{L}^{\text{orth}}(g, \eta^0)$ is minimized by any scoring function of the form*

$$g(x) = \frac{1}{\kappa} \tau^0(x) + c, \quad (16)$$

for some constant $c \in \mathbb{R}$, and therefore recovers the treatment effect ordering.

Proof. See Appendix D.

Together, Theorem 5.1 (Neyman-orthogonality) and Theorem 5.2 (correct population minimizers)³ establish that $\mathcal{L}^{\text{orth}}(g, \eta)$ targets the correct treatment effect ordering while remaining robust to nuisance estimation errors. Table 2 summarizes the four considered learning objectives, their population optima, the induced constraints on g , and whether they are Neyman-orthogonal.

Intuition of the pseudo labels. Intuitively, the pseudo labels in Eq. (12) can be viewed as the soft ranking targets augmented with an orthogonal correction. Note that the correction term itself is the product of (i) an uncertainty-dependent weight ω_τ and (ii) a difference of doubly robust scores Δ_η . Hence, when the (plug-in) soft target is close to 0 or 1, the implied pairwise ordering of treatment effects is non-ambiguous and the weight is small, so the pseudo label remains close to the soft target. In contrast, when the soft target is near 0.5, the pairwise ordering tends to be ambiguous and the weight becomes large, thus activating the correction and shifting the pseudo label according to the doubly robust score difference.

The smoothness parameter κ controls *when* and *how strongly* this correction is applied through the weight in Eq. (13). Here, smaller values of κ sharpen the soft targets, pushing them closer to 0 or 1 and reducing the number of pairs for which the correction is active. At the same time, for the remaining ambiguous pairs, the correction weight increases due to the $(1/\kappa)$ scaling. As a result, the orthogonal correction concentrates on fewer, harder pairs, but with a larger impact on their pseudo labels.

Behavior of the orthogonal ranking loss. The population minimizers of the orthogonal loss $\mathcal{L}^{\text{orth}}$ in Eq. (16) require learning a scaled version of the CATE function up to an additive constant, with a scaling factor of $(1/\kappa)$. As the smoothness parameter $\kappa \rightarrow 0$, this scaling factor diverges and the minimizer becomes unbounded. At the same time, decreasing κ also changes the *shape* of the loss around the optimum. The loss becomes increasingly flat along directions that preserve the treatment effect ordering: deviations of a candidate scoring function g from the population minimizers that do not change the induced ranking are only weakly penalized. This behavior reflects that, in this limit, the orthogonal loss $\mathcal{L}^{\text{orth}}$ approaches the binary ranking loss \mathcal{L}^{bin} , which recovers only the ordering of treatment effects and does not admit a finite population minimizer (see Appendix D.2 for details).

Consequently, smaller values of κ progressively reduce the learning objective from recovering the full shape of the CATE towards a pure ranking problem. As discussed above, decreasing κ also amplifies the orthogonal correction for

³Note that $\mathcal{L}^{\text{orth}}$ and $\mathcal{L}^{\text{soft}}$ share the same set of population minimizers; for details see Appendix D.

Learning objective	Population optimum	Constraint on g (intuition)	Orthogonal
$\mathcal{L}^{\text{cate}}(g, \eta) = \mathbb{E}[(g(X) - \tau(X))^2]$	$g(x) = \tau(x)$	Identifies the full CATE function (learns magnitudes).	✗
$\mathcal{L}^{\text{bin}}(g, \eta) = \mathbb{E}[\ell(p_g(X, X'), b_\tau(X, X'))]$	$g(x) = h(\tau(x))$ with h strictly increasing	Identifies the CATE ordering (learns ranking, not magnitudes).	✗
$\mathcal{L}^{\text{soft}}(g, \eta) = \mathbb{E}[\ell(p_g(X, X'), t_\tau(X, X'))]$		Identifies a scaled CATE up to a shift (interpolates between ranking and magnitudes via parameter κ).	✗
$\mathcal{L}^{\text{orth}}(g, \eta) = \mathbb{E}[\ell(p_g(X, X'), \tilde{t}_\eta(W, W'))]$	$g(x) = \frac{1}{\kappa} \tau(x) + c$		✓

Table 2. Summary of learning objectives. We compare four learning objectives, their population optima evaluated at the true nuisance functions, the induced constraints on the scoring function g , and whether they are Neyman-orthogonal. For \mathcal{L}^{bin} , the “optimum” denotes the class of order-preserving scoring functions that can approach the infimum arbitrarily closely (not attainable by any finite g). Our proposed orthogonal objective is highlighted.

pairs with similar treatment effects, which increases the variability of the pseudo labels in finite samples. The choice of κ therefore reflects a bias-variance trade-off; we propose a practical strategy for selecting the value in the next section.

6. Rank-Learner: A two-stage learner for ranking treatment effects

In this section, we introduce *Rank-Learner*, an orthogonal two-stage learner for ranking individuals by their treatment effects from observational data. *Rank-Learner* proceeds as follows. ① In the first stage, we estimate nuisance functions $\hat{\eta}$ via cross-fitting using flexible machine learning models. ② In the second stage, we fit a scoring function g by minimizing the empirical orthogonal ranking objective $\mathcal{L}^{\text{orth}}(g, \hat{\eta})$ on a random subsample of the training pairs. ③ At inference time, the scoring function \hat{g} can be used directly to rank individuals, without having to perform any pairwise comparisons. An overview of our *Rank-Learner* is shown in Figure 2; we now describe each stage in detail.

① Nuisance estimation. In the first stage, we estimate the nuisance functions $\hat{\eta} = (\hat{\mu}_1, \hat{\mu}_0, \hat{e})$, with $\mu_t(x)$ the response surfaces and $e(x)$ the propensity score, using flexible machine learning models. Following standard practice in orthogonal learning, we use cross-fitted estimates $\hat{\eta}$ in the second-stage (Chernozhukov et al., 2018).

② Orthogonal learning. In the second stage, we train a scoring function g by minimizing the empirical objective

$$\mathcal{L}^{\text{orth}}(g, \hat{\eta}) = \frac{1}{|\mathcal{P}|} \sum_{(i,j) \in \mathcal{P}} \ell(p_g(x_i, x_j), \tilde{t}_{\hat{\eta}}(w_i, w_j)) \quad (17)$$

where \mathcal{P} is the set of sampled training pairs. For each pair $(i, j) \in \mathcal{P}$, the pairwise prediction of the model is $p_g(x_i, x_j)$ and the corresponding pseudo label is $\tilde{t}_{\hat{\eta}}(w_i, w_j)$. Importantly, orthogonality is incorporated *entirely* through these pseudo labels, while the loss itself retains the standard binary cross-entropy form. Consequently, the second-stage learning problem remains identical to standard pairwise

ranking, up to the construction of the training labels.

Since a dataset of size n induces $|\mathcal{P}_{\text{all}}| = n^2$ possible training pairs, the second-stage optimization can become prohibitively expensive. To scale *Rank-Learner*, we therefore propose to optimize the loss using only a random subsample of pairs $\mathcal{P} \subset \mathcal{P}_{\text{all}}$ in each epoch, drawn uniformly from all available pairs. In our experiments, we show that ranking performance saturates quickly as the number of sampled pairs increases, suggesting that only a small fraction of pairs is usually sufficient.

We select κ by maximizing an out-of-sample ranking criterion on a validation set. Concretely, we use the *area under the targeting operator curve* (AUTOC), which measures the average benefit of treating units in the order induced by a score (here \hat{g}), averaged across all treatment fractions (Yadlowsky et al., 2025). Since the AUTOC depends on unobserved treatment effects, we rely on the approximation proposed by Chernozhukov et al. (2025). The remaining hyperparameters are tuned analogously (see Appendix E.3).

③ Inference. The output of the second stage is a fitted scoring function $\hat{g} : \mathcal{X} \rightarrow \mathbb{R}$. Given a target population $\{x_i\}_{i=1}^m$, we compute scores $\hat{g}(x_i)$ and rank individuals accordingly, with larger values indicating higher predicted priority (i.e., a larger treatment effect in the induced ordering). Pairwise comparisons are only needed during training, since inference requires only pointwise evaluation of \hat{g} . For implementation details, see Appendix E.3.

7. Experiments

We evaluate *Rank-Learner* on both synthetic and semi-synthetic benchmarks where ground-truth treatment effects are available, following standard practice in the causal inference literature (Kamran et al., 2024; Kennedy, 2023; Curth & van der Schaar, 2021; Shalit et al., 2017). The full data-generating processes and additional experimental results are provided in Appendix E.

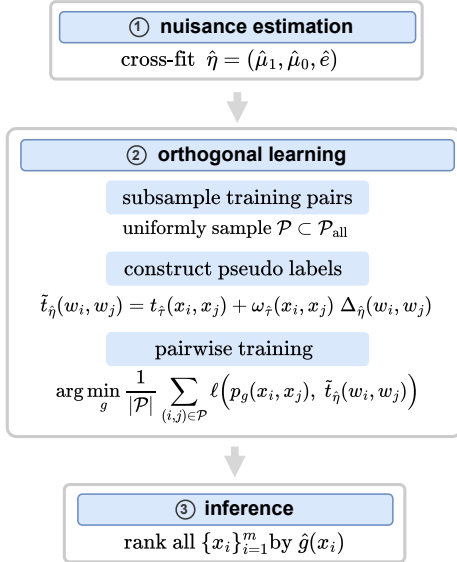


Figure 2. Overview of Rank-Learner. In the first stage, we estimate nuisance functions (response surfaces and propensity score) via cross-fitting. In the second stage, we subsample training pairs, construct the pseudo labels, and learn a scoring function by minimizing the orthogonal ranking objective. Both stages can be instantiated with arbitrary machine learning models. At inference time, we rank individuals directly by their learned scores $\hat{g}(x)$.

7.1. Experimental design

Setup. In all benchmarks, we generate treatment effects as a strictly increasing, non-linear transformation of a latent score $s(x)$, such that the ground-truth ranking is fully determined by $s(x)$, while the treatment effect magnitudes depend on the chosen transformation. In the semi-synthetic setting, we use real covariates from established datasets covering distinct application domains – MOVIELENS (recommender systems), MIMIC-III (healthcare), and the CURRENT POPULATION SURVEY (public policy) – but construct treatments and outcomes following the same design principles as in the synthetic benchmark (Harper & Konstan, 2015; Johnson et al., 2016; Flood et al., 2025). For further details, we refer to Appendix E.1 and E.2.

Across all experiments, we evaluate on a fixed test set of 1,000 samples and report results over five seeds. On the synthetic benchmark, we vary the training size from $n = 100$ to $n = 2,000$ to study ranking performance as a function of data availability. To separate nuisance estimation and second-stage learning, we use sample splitting: one sample of size n is used to fit the nuisance functions, and an independent sample of the same size n is used to train the second-stage models (each with an internal train/validation split). In the semi-synthetic setting, we fix the training size to $n = 1,000$ and follow the same protocol. Tables report mean \pm standard deviation over seeds, while figures show mean \pm standard error.

Baselines and training details. We compare *Rank-Learner* against the naïve CATE-based strategy using the **T-learner** (Künzel et al., 2019) and the **DR-learner** (Kennedy, 2023), with the latter being Neyman-orthogonal. To isolate the benefit of orthogonalization for ranking, we also include a non-orthogonal **plug-in ranker** that learns a scoring model g by optimizing $\mathcal{L}^{\text{soft}}(g, \hat{\eta})$. This learning objective uses the soft targets, based on plug-in estimates of the treatment effects, instead of the orthogonal pseudo labels. These baselines allow us to disentangle (i) the benefit of direct ranking versus the naïve strategy based on *full* CATE estimation and (ii) orthogonal versus plug-in objectives for ranking.

Across all experiments, we use the *same* model architecture and training details for a *fair* comparison. In particular, the nuisance functions and second-stage models are implemented as feedforward neural networks with a single hidden layer and ReLU activations, with linear output layers for regression and sigmoid output layers for classification. Models are trained with Adam (Kingma & Ba, 2015) for up to 50 epochs, with early stopping based on the validation loss, retaining the best model checkpoint. For model selection, we tune the hyperparameters of the ranking methods using the approximated AUTOC on the validation set (Chernozhukov et al., 2025), while CATE estimators are selected using their standard validation loss. Training is computationally lightweight with all models converging within minutes. Further implementation details are in Appendix E.3.

Evaluation metrics. Our primary evaluation metric is the AUTOC (Yadlowsky et al., 2025). The AUTOC evaluates how well a method ranks individuals by treatment effects by averaging the cumulative treatment benefit among the top-ranked individuals, over all fractions. In our evaluation, we compute AUTOC on the test set using the ground-truth treatment effects. Unlike AUROC, AUTOC is not normalized and therefore not constrained to $[0, 1]$. For completeness, we also report the *mean policy value* in Appendix F, which evaluates the quality of the implied policies.

7.2. Synthetic benchmark results

Table 3 reports test AUTOC across training sizes on the synthetic benchmark. We draw three main findings. (1) *Rank-Learner* consistently outperforms standard pointwise CATE estimators (T- and DR-learners) across all sample sizes, demonstrating the benefit of directly targeting treatment effect ranking rather than recovering effect magnitudes. (2) Compared to the non-orthogonal plug-in ranker, *Rank-Learner* achieves systematically higher AUTOC, with the largest improvements observed in small-sample regimes where nuisance estimation error is most pronounced. This highlights the advantage of orthogonalization for ranking. (3) As training size increases, performance differences across methods become smaller, reflecting improved

Table 3. Synthetic benchmark (main results): Test AUTOCC (mean \pm std dev over five seeds) across training sizes. *Higher is better*. The oracle column reports AUTOCC obtained by ranking the test set using the true treatment effects. Best mean is shown in **bold**.

Method	$n = 100$	$n = 250$	$n = 500$	$n = 1,000$	$n = 2,000$	oracle
T-learner	0.88 ± 0.17	0.96 ± 0.14	1.24 ± 0.05	1.32 ± 0.02	1.36 ± 0.00	
DR-learner	0.80 ± 0.18	1.16 ± 0.12	1.28 ± 0.05	1.33 ± 0.02	1.36 ± 0.02	
Plug-in ranker	0.69 ± 0.32	0.95 ± 0.14	1.24 ± 0.06	1.31 ± 0.02	1.36 ± 0.00	
Rank-learner (ours)	0.94 ± 0.21	1.28 ± 0.03	1.30 ± 0.03	1.34 ± 0.01	1.37 ± 0.00	1.40

nuisance estimation quality in our controlled setting (Appendix F, Table 6). Importantly, the relative ordering of methods remains unchanged, with *Rank-Learner* achieving the strongest performance throughout. Taken together, these results show that, among the considered baselines, directly targeting the ranking task with an orthogonal learning objective yields the best performance.

Pair subsampling. Figure 3 shows the computational trade-off from subsampling training pairs in the second-stage ranker, and its effect on ranking performance. *Rank-Learner* attains strong performance in terms of AUTOCC, even when using only a small fraction of pairs per epoch. This suggests that the second-stage performance is mostly driven by the quality of the nuisance estimates, and that subsampling is an effective way to scale our *Rank-Learner*.

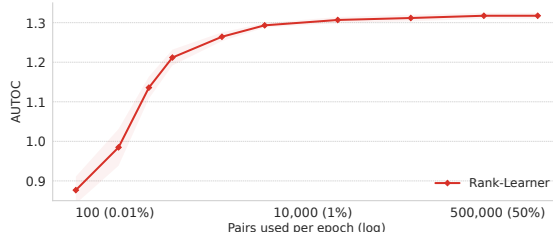


Figure 3. Synthetic benchmark (pair subsampling). Test AUTOCC (mean \pm s.e. over five seeds) of *Rank-Learner* as a function of the number of sampled training pairs per epoch ($n = 1,000$ with $n^2 = 10^6$ possible training pairs). *Higher is better*. The horizontal axis shows the fraction of pairs used (log).

Sensitivity to overlap. Figure 4 studies the robustness to limited overlap by varying the propensity mechanism while keeping the remaining components of the synthetic data-generating process fixed (see Appendix F for details). As overlap decreases, ranking performance deteriorates for all methods, which is expected and reflects the increasing difficulty of causal inference when treated and control groups become less comparable. Importantly, across the full range of overlap levels considered, our *Rank-Learner* consistently achieves the highest mean AUTOCC.

Additional results. Additional results are reported in Appendix F. In particular, Table 7 includes a comparison to the *tree ranker* of Kamran et al. (2024), where *Rank-Learner* performs best overall.

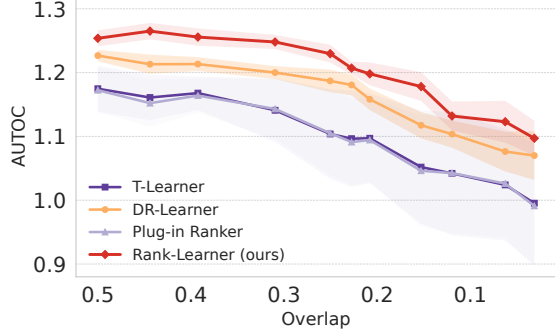


Figure 4. Synthetic benchmark (overlap sensitivity). Test AUTOCC (mean \pm s.e. over five seeds) as a function of overlap (decreasing left to right) for $n = 500$. *Higher is better*. Overlap is varied by changing treatment assignment, remaining components of the synthetic data-generating process are kept fixed.

7.3. Semi-synthetic benchmark results

We next evaluate *Rank-Learner* on the three semi-synthetic benchmarks with realistic covariate distributions (MOVIELENS, MIMIC-III, and CPS). This experiment tests whether the benefits of orthogonal ranking extend beyond synthetic data. Table 4 reports test AUTOCC at a fixed training size of $n = 1,000$. At this sample size, nuisance estimation error remains considerable, mirroring the difficulty of learning nuisance functions from observational data. Across all datasets, *Rank-Learner* achieves the strongest ranking performance among the considered baselines, with consistent improvements over the plug-in ranker and the pointwise CATE estimators.

Table 4. Semi-synthetic benchmarks: Test AUTOCC (mean \pm std dev over five seeds) with training size $n = 1,000$. *Higher is better*. The oracle row reports AUTOCC obtained by ranking the test set using the true treatment effects. Best mean is shown in **bold**.

Method	MOVIELENS	MIMIC-III	CPS
oracle	1.39	1.22	1.01
T-learner	1.31 ± 0.03	1.12 ± 0.05	0.87 ± 0.08
DR-learner	1.34 ± 0.02	1.16 ± 0.02	0.92 ± 0.02
Plug-in ranker	1.30 ± 0.03	1.11 ± 0.05	0.87 ± 0.08
Rank-learner (ours)	1.35 ± 0.01	1.18 ± 0.02	0.95 ± 0.01

Conclusion. We introduced *Rank-Learner*, the first Neyman-orthogonal two-stage learner for ranking individuals by their treatment effects from observational data.

Impact statement

This paper presents methodological work aimed at advancing the field of machine learning and causal inference. While ranking individuals by treatment effects may inform decision-making in domains such as healthcare, marketing, or public policy, the proposed method is not tied to any specific application. As with all causal methods based on observational data, responsible use requires careful consideration of the underlying assumptions (e.g., unconfoundedness) and the context in which the estimates / rankings are applied.

Acknowledgments

This paper is supported by the DAAD programme Konrad Zuse Schools of Excellence in Artificial Intelligence, sponsored by the Federal Ministry of Research, Technology and Space. This research also received funding from the Research Foundation Flanders (FWO Vlaanderen) with grant number 11Q2C24N and from the Flemish government under the “Onderzoeksprogramma Artificiële Intelligentie (AI) Vlaanderen” programme.

References

Aquino, Y. S. J., Rogers, W., Scully, J. L., Magrabi, F., and Carter, S. Ethical guidance for hard decisions: A critical review of early international COVID-19 ICU triage guidelines. *Health Care Analysis*, 30(2):163–195, 2022.

Athey, S. and Wager, S. Policy learning with observational data. *Econometrica*, 89(1):133–161, 2021.

Burges, C., Shaked, T., Renshaw, E., Lazier, A., Deeds, M., Hamilton, N., and Hullender, G. Learning to rank using gradient descent. In *International Conference on Machine Learning (ICML)*, 2005.

Buyl, M., Missault, P., and Sondag, P.-A. RankFormer: Listwise learning-to-rank using listwide labels. In *Conference on Knowledge Discovery and Data Mining (KDD)*, 2023.

Cao, Z., Qin, T., Liu, T.-Y., Tsai, M.-F., and Li, H. Learning to rank: From pairwise approach to listwise approach. In *International Conference on Machine Learning (ICML)*, 2007.

Card, D., Klue, J., and Weber, A. What works? A meta analysis of recent active labor market program evaluations. *Journal of the European Economic Association*, 16 (3):894–931, 2018.

Chernozhukov, V., Chetverikov, D., Demirer, M., Duflo, E., Hansen, C., Newey, W., and Robins, J. Double/debiased machine learning for treatment and structural parameters. *The Econometrics Journal*, 21(1):C1–C68, 2018.

Chernozhukov, V., Hansen, C., Kallus, N., Spindler, M., and Syrgkanis, V. *Causal Inference with ML and AI*. Online, 2025.

Curth, A. and van der Schaar, M. Nonparametric estimation of heterogeneous treatment effects: From theory to learning algorithms. In *International Conference on Artificial Intelligence and Statistics (AISTATS)*, 2021.

Devriendt, F., Berrevoets, J., and Verbeke, W. Why you should stop predicting customer churn and start using uplift models. *Information Sciences*, 548:497–515, 2021.

Flood, S., King, M., Rodgers, R., Ruggles, S., Warren, R., Backman, D., Breton, E., Cooper, G., Rivera Drew, J., Richards, S., Van Riper, D., and Williams, K. IPUMS CPS, 2025. URL <https://cps.ipums.org/cps/>.

Foster, D. and Syrgkanis, V. Orthogonal statistical learning. *The Annals of Statistics*, 51(3):879–908, 2023.

Frauen, D., Melnychuk, V., and Feuerriegel, S. Fair off-policy learning from observational data. In *International Conference on Machine Learning (ICML)*, 2024.

Frauen, D., Melnychuk, V., Schweisthal, J., van der Schaar, M., and Feuerriegel, S. Treatment effect estimation for optimal decision-making. In *Neural Information Processing Systems (NeurIPS)*, 2025.

Gharibshah, Z. and Zhu, X. User response prediction in online advertising. *ACM Computing Surveys*, 54(3):64:1–64:43, 2021.

Harper, M. and Konstan, J. The MovieLens datasets: History and context. *ACM Transactions on Interactive Intelligent Systems*, 5(4):19:1–19:19, 2015.

Hess, K., Frauen, D., Melnychuk, V., and Feuerriegel, S. Efficient and sharp off-policy learning under unobserved confounding. In *International Conference for Learning Representations (ICLR)*, 2026.

Hines, O., Dukes, O., Diaz-Ordaz, K., and Vansteelandt, S. Demystifying statistical learning based on efficient influence functions. *The American Statistician*, 76(3):292–304, 2022.

Imbens, G. and Rubin, D. *Causal Inference for Statistics, Social, and Biomedical Sciences: An Introduction*. Cambridge University Press, Cambridge, 2015.

Johnson, A., Pollard, T., Shen, L., Lehman, L.-W., Feng, M., Ghassemi, M., Moody, B., Szolovits, P., Anthony Celi, L., and Mark, R. MIMIC-III, a freely accessible critical care database. *Scientific Data*, 3(1):160035, 2016.

Kallus, N. Balanced policy evaluation and learning. In *Neural Information Processing Systems (NeurIPS)*, 2018.

Kallus, N. More efficient policy learning via optimal retargeting. *Journal of the American Statistical Association*, 116(534):646–658, 2021.

Kamran, F., Makar, M., and Wiens, J. Learning to rank for optimal treatment allocation under resource constraints. In *International Conference on Artificial Intelligence and Statistics (AISTATS)*, 2024.

Kennedy, E. Towards optimal doubly robust estimation of heterogeneous causal effects. *Electronic Journal of Statistics*, 17(2):3008–3049, 2023.

Kennedy, E. Semiparametric doubly robust targeted double machine learning: A review. In *Handbook of Statistical Methods for Precision Medicine*. 2024.

Kingma, D. and Ba, J. Adam: A method for stochastic optimization. In *International Conference for Learning Representations (ICLR)*, 2015.

Kraus, M., Feuerriegel, S., and Saar-Tsechansky, M. Data-driven allocation of preventive care with application to diabetes mellitus type II. *Manufacturing & Service Operations Management*, 26(1):137–153, 2024.

Künzel, S., Sekhon, J., Bickel, P., and Yu, B. Metalearners for estimating heterogeneous treatment effects using machine learning. *Proceedings of the National Academy of Sciences*, 116(10):4156–4165, 2019.

Liu, T.-Y. *Learning to Rank for Information Retrieval*. Springer, Berlin, Heidelberg, 2011.

Morzywolek, P., Decruyenaere, J., and Vansteelandt, S. On weighted orthogonal learners for heterogeneous treatment effects, 2024.

Nie, X. and Wager, S. Quasi-oracle estimation of heterogeneous treatment effects. *Biometrika*, 108(2):299–319, 2021.

Qian, M. and Murphy, S. Performance guarantees for individualized treatment rules. *The Annals of Statistics*, 39(2):1180–1210, 2011.

Rosenbaum, P. and Rubin, D. The central role of the propensity score in observational studies for causal effects. *Biometrika*, 70(1):41–55, 1983.

Rubin, D. Causal inference using potential outcomes: Design, modeling, decisions. *Journal of the American Statistical Association*, 100(469):322–331, 2005.

Schweisthal, J., Frauen, D., Melnychuk, V., and Feuerriegel, S. Reliable off-policy learning for dosage combinations. In *Neural Information Processing Systems (NeurIPS)*, 2023.

Shalit, U., Johansson, F., and Sontag, D. Estimating individual treatment effect: Generalization bounds and algorithms. In *International Conference on Machine Learning (ICML)*, pp. 3076–3085, 2017.

Vanderschueren, T., Verbeke, W., Moraes, F., and Proen  a, H. M. Metalearners for ranking treatment effects, 2024.

Vinay, R., Baumann, H., and Biller-Andorno, N. Ethics of ICU triage during COVID-19. *British Medical Bulletin*, 138(1):5–15, 2021.

Wager, S. and Athey, S. Estimation and inference of heterogeneous treatment effects using random forests. *Journal of the American Statistical Association*, 113(523):1228–1242, 2018.

Yadlowsky, S., Fleming, S., Shah, N., Brunskill, E., and Wager, S. Evaluating treatment prioritization rules via rank-weighted average treatment effects. *Journal of the American Statistical Association*, 120(549):38–51, 2025.

A. Extended literature review on policy learning

In policy learning, the aim is to learn a treatment assignment rule $\pi : \mathcal{X} \rightarrow \{0, 1\}$ from observational data that maximizes the so-called *policy value* $V(\pi) = \mathbb{E}[Y(\pi(X))]$, which represents the mean outcome in the population under the policy $\pi(x)$. There has been extensive work on this topic (Qian & Murphy, 2011), including methods designed for limited overlap (Kallus, 2021; 2018) and for unobserved confounding (Hess et al., 2026), doubly-robust methods (Athey & Wager, 2021), extensions to continuous treatments (Schweisthal et al., 2023), fairness-constrained policies (Frauen et al., 2024), and interpretable CATE-based policies (Frauen et al., 2025). In the unconstrained case, an *optimal* policy treats everyone in the target population with $\tau(x) > 0$, whereas, in the constrained case, it treats only the top-ranked individuals by $\tau(x)$, which motivates learning policies over restricted function classes.

However, our goal is not to learn a *binary* treatment policy, but to learn a real-valued scoring function $g(x)$ that can be used to rank individuals by their treatment effects. Unlike policy learning, our target is *threshold-independent*: we aim to recover a global ordering rather than learning a specific policy given a fixed budget or constraint. Hence, contrarily, a single learned ranking under our *Rank-Learner* could even be used downstream to instantiate different treatment policies (e.g., for different treatment budgets or constraints), without having to retrain the model for each choice.

B. Orthogonal learning based on influence functions

In this appendix, we provide a brief background on influence functions and how they can be used to construct orthogonal losses following [Kennedy \(2024\)](#).

Influence functions. We consider a setting where we observe data $W = (X, T, Y)$ distributed according to an unknown probability distribution \mathbb{P} that lies in some statistical model \mathcal{P} (a set of distributions). The goal is to estimate a statistical quantity of interest that can be expressed as a functional $\psi : \mathcal{P} \rightarrow \mathbb{R}$ (as an example, consider the average treatment effect $\psi(\mathbb{P}) = \mathbb{E}_X [\mathbb{E}[Y | T = 1, X] - \mathbb{E}[Y | T = 0, X]]$). Intuitively, the influence function $\text{IF}_\psi(w, \mathbb{P})$ captures the sensitivity of the target functional to small perturbations of the distribution \mathbb{P} , obtained by adding an infinitesimal amount of probability mass on the observation $W = w$.

Plug-in bias and the one-step correction. A natural way to estimate the functional of interest is to directly replace the true distribution \mathbb{P} with a finite-sample estimate $\hat{\mathbb{P}}$ to obtain the *plug-in* estimator $\psi(\hat{\mathbb{P}})$. However, since $\hat{\mathbb{P}}$ only approximates \mathbb{P} , plug-in estimators typically suffer from a first-order bias term that can be expressed through the influence function

$$\psi(\hat{\mathbb{P}}) - \psi(\mathbb{P}) = - \int \text{IF}_\psi(w, \hat{\mathbb{P}}) d\mathbb{P}(w) + R_2, \quad (18)$$

where R_2 collects higher-order remainder terms that are negligible under mild conditions. This implies that simply “plugging-in” an estimate of the distribution \mathbb{P} into the functional ψ yields a biased estimator. In order to correct this bias, the term involving the influence function can be estimated from the sample and added back to the plug-in estimator, resulting in the one-step corrected estimator

$$\hat{\psi}^{\text{one-step}} = \psi(\hat{\mathbb{P}}) + \mathbb{P}_n [\text{IF}_\psi(W, \hat{\mathbb{P}})]. \quad (19)$$

Orthogonal loss construction. In this work, the goal is *not* to estimate a finite-dimensional target parameter such as the average treatment effect. Instead, we aim to learn a model $g(x)$ that preserves the ranking induced by the conditional average treatment effect $\tau(x)$, which is an infinite-dimensional quantity. Therefore, the one-step correction described above is not directly applicable to our setting. However, the population loss $\mathcal{L}(g, \eta)$ that is used to learn g depends on unknown nuisance components $\eta = (\mu_1, \mu_0, e)$, which each depend on \mathbb{P} . In practice, these components must be replaced by estimates $\mathcal{L}(g, \hat{\eta})$, which introduce the same kind of *plug-in bias* as in the standard setting with a finite-dimensional target quantity. By applying the correction based on the influence function directly to the loss, we obtain an orthogonal loss whose gradients are first-order insensitive to estimation errors in the nuisances (i.e., Neyman-orthogonality; see Section 4 for a background).

C. Derivation and proof of the Neyman-orthogonal ranking loss

In Appendix B, we gave the intuition behind orthogonal learning based on influence functions and why it is desirable in our setting. In this appendix, we formally derive our proposed loss and prove that it is Neyman-orthogonal.

C.1. Derivation of the efficient influence function

Strategy. In order to derive the efficient influence function of our loss, we follow the strategy proposed by [Kennedy \(2024\)](#) and [Hines et al. \(2022\)](#). We work with a nonparametric statistical model \mathcal{P} , defined as the set of all probability distributions for the observed data $W = (X, T, Y)$. Let $\mathbb{P} \in \mathcal{P}$ denote the true data-generating distribution of W and consider the one-dimensional parametric submodel

$$\mathcal{P}_\epsilon = \{\mathbb{P}_\epsilon = (1 - \epsilon)\mathbb{P} + \epsilon\delta_w \mid \epsilon \in [0, 1]\}, \quad \text{with } \mathcal{P}_\epsilon \subseteq \mathcal{P}, \quad (20)$$

where δ_w denotes a point-mass distribution that assigns all its probability mass to the observation $W = w$. For this choice of submodel, the influence function of any functional $\psi(\mathbb{P})$ is given by the directional derivative

$$\mathbb{IF}_\psi(w, \mathbb{P}) = \left. \frac{d}{d\epsilon} \psi(\mathbb{P}_\epsilon) \right|_{\epsilon=0}. \quad (21)$$

This characterization allows us to derive the efficient influence function of our loss by differentiating $\psi(\mathbb{P}_\epsilon) = \mathcal{L}(g, \eta_\epsilon)$ with respect to ϵ . This can be carried out by using standard differentiation rules and by treating the expectations inside $\mathcal{L}(g, \eta_\epsilon)$ as finite sums, as if the data were discrete. For a comprehensive background and technical details, we refer to [\(Kennedy, 2024\)](#) and [\(Hines et al., 2022\)](#).

Derivation. Recall that our goal is to learn a scoring function $g(x)$ that preserves the ordering induced by the conditional average treatment effect $\tau(x)$. To this end, we consider the pairwise population loss

$$\mathcal{L}^{\text{soft}}(g, \eta) = \mathbb{E}_{X, X'} \left[\ell(p_g(X, X'), t_\tau(X, X')) \right] \quad (22)$$

$$= \mathbb{E}_{X, X'} \left[-t_\tau(X, X') \log p_g(X, X') - (1 - t_\tau(X, X')) \log (1 - p_g(X, X')) \right], \quad (23)$$

where $\ell(p, t) = -t \log p - (1 - t) \log(1 - p)$ denotes the binary cross-entropy loss. For brevity, we sometimes write $\ell(X, X')$ to denote $\ell(p_g(X, X'), t_\tau(X, X'))$, where we use

$$p_g(X, X') = \sigma(g(X) - g(X')), \quad \text{and} \quad t_\tau(X, X') = \sigma\left(\frac{\tau(X) - \tau(X')}{\kappa}\right). \quad (24)$$

Here, $\kappa > 0$ is a smoothness parameter, and the nuisance components η enter the loss through $\tau(X) = \mu_1(X) - \mu_0(X)$.

The influence function of this loss evaluated at $w_0 = (x_0, t_0, y_0)$ can be written based on the product rule as

$$\mathbb{IF}_{\mathcal{L}^{\text{soft}}}(w_0, \mathbb{P}) = \underbrace{\sum_x \sum_{x'} \mathbb{IF}_{\ell(x, x')}(w_0, \mathbb{P}) p(x)p(x')}_{A(w_0, \mathbb{P})} + \underbrace{\sum_x \sum_{x'} \ell(x, x') \mathbb{IF}_{p(x)p(x')}(w_0, \mathbb{P})}_{B(w_0, \mathbb{P})}. \quad (25)$$

Considering the $A(w_0, \mathbb{P})$ term, for fixed (x, x') , the dependence of $\ell(x, x')$ on \mathbb{P} is only through $t_\tau(x, x')$, and by the chain rule we have

$$\mathbb{IF}_{\ell(x, x')}(w_0, \mathbb{P}) = \frac{\partial \ell(x, x')}{\partial t_\tau(x, x')} \frac{\partial t_\tau(x, x')}{\partial (\tau(x) - \tau(x'))} \mathbb{IF}_{\tau(x) - \tau(x')}(w_0, \mathbb{P}) \quad (26)$$

$$= \underbrace{\log\left(\frac{1 - p_g(x, x')}{p_g(x, x')}\right)}_{C(x, x')} \underbrace{\left(\frac{t_\tau(x, x')(1 - t_\tau(x, x'))}{\kappa}\right)}_{\mathbb{IF}_{\tau(x)}(w_0, \mathbb{P}) - \mathbb{IF}_{\tau(x')}(w_0, \mathbb{P})} \quad (27)$$

$$= C(x, x') \left(\mathbb{IF}_{\tau(x)}(w_0, \mathbb{P}) - \mathbb{IF}_{\tau(x')}(w_0, \mathbb{P}) \right). \quad (28)$$

To evaluate the term $\mathbb{IF}_{\tau(x)}(w_0, \mathbb{P})$, we use the known influence function of the CATE at a fixed covariate value x , given by

$$\mathbb{IF}_{\tau(x)}(w_0, \mathbb{P}) = \frac{\mathbf{I}\{x_0 = x\}}{p(x)} \left(\frac{t_0}{e(x)} (y_0 - \mu_1(x)) - \frac{1 - t_0}{1 - e(x)} (y_0 - \mu_0(x)) \right) \quad (29)$$

$$= \frac{\mathbf{I}\{x_0 = x\}}{p(x)} (\phi_\eta(w_0, x) - \tau(x)), \quad (30)$$

where the last line is obtained by adding and subtracting $\tau(x)$, and denoting $\phi_\eta(w_0, x)$ the doubly robust score for $\tau(x)$, which depends on the nuisances $\eta = (\mu_1, \mu_0, e)$. Plugging this into the expression for $A(w_0, \mathbb{P})$, we get

$$\begin{aligned} A(w_0, \mathbb{P}) &= \sum_x \sum_{x'} C(x, x') \mathbf{I}\{x_0 = x\} (\phi_\eta(w_0, x) - \tau(x)) p(x') \\ &\quad - \sum_x \sum_{x'} C(x, x') \mathbf{I}\{x_0 = x'\} (\phi_\eta(w_0, x') - \tau(x')) p(x) \end{aligned} \quad (31)$$

$$= \sum_{x'} C(x_0, x') (\phi_\eta(w_0, x_0) - \tau(x_0)) p(x') - \sum_x C(x, x_0) (\phi_\eta(w_0, x_0) - \tau(x_0)) p(x) \quad (32)$$

$$= \mathbb{E}_{X'} [C(x_0, X')] (\phi_\eta(w_0) - \tau(x_0)) - \mathbb{E}_X [C(X, x_0)] (\phi_\eta(w_0) - \tau(x_0)), \quad (33)$$

where for brevity we write $\phi_\eta(w_0)$ rather than $\phi_\eta(w_0, x_0)$, since $w_0 = (x_0, t_0, y_0)$ already contains the covariates x_0 on which the score depends.

Now consider the $B(w_0, \mathbb{P})$ term, where, by the product rule, we have

$$B(w_0, \mathbb{P}) = \sum_x \sum_{x'} \ell(x, x') \mathbb{IF}_{p(x)p(x')}(w_0, \mathbb{P}) \quad (34)$$

$$= \sum_x \sum_{x'} \ell(x, x') \mathbb{IF}_{p(x)}(w_0, \mathbb{P}) p(x') + \sum_x \sum_{x'} \ell(x, x') p(x) \mathbb{IF}_{p(x')}(w_0, \mathbb{P}). \quad (35)$$

To evaluate the term $\mathbb{IF}_{p(x)}(w_0, \mathbb{P})$, we use the known influence function of a marginal distribution at a fixed covariate value x , given by

$$\mathbb{IF}_{p(x)}(w_0, \mathbb{P}) = \mathbf{I}\{x_0 = x\} - p(x). \quad (36)$$

Plugging this into the equation for $B(w_0, \mathbb{P})$ gives

$$B(w_0, \mathbb{P}) = \sum_x \sum_{x'} \ell(x, x') \mathbf{I}\{x_0 = x\} p(x') - \sum_x \sum_{x'} \ell(x, x') p(x) p(x') \quad (37)$$

$$\begin{aligned} &\quad + \sum_x \sum_{x'} \ell(x, x') \mathbf{I}\{x_0 = x'\} p(x) - \sum_x \sum_{x'} \ell(x, x') p(x) p(x') \\ &= \mathbb{E}_{X'} [\ell(x_0, X')] - \mathbb{E}_{X, X'} [\ell(X, X')] + \mathbb{E}_X [\ell(X, x_0)] - \mathbb{E}_{X, X'} [\ell(X, X')]. \end{aligned} \quad (38)$$

Putting everything together, the efficient influence function of the population loss $\mathcal{L}^{\text{soft}}$ becomes

$$\mathbb{IF}_{\mathcal{L}^{\text{soft}}}(w_0, \mathbb{P}) = A(w_0, \mathbb{P}) + B(w_0, \mathbb{P}) \quad (39)$$

$$= \mathbb{E}_{X'} [C(x_0, X')] (\phi_\eta(w_0) - \tau(x_0)) - \mathbb{E}_X [C(X, x_0)] (\phi_\eta(w_0) - \tau(x_0)) \quad (40)$$

$$+ \mathbb{E}_{X'} [\ell(x_0, X')] - \mathbb{E}_{X, X'} [\ell(X, X')] + \mathbb{E}_X [\ell(X, x_0)] - \mathbb{E}_{X, X'} [\ell(X, X')],$$

with

$$C(x, x') = \log \left(\frac{1 - p_g(x, x')}{p_g(x, x')} \right) \left(\frac{t_\tau(x, x') (1 - t_\tau(x, x'))}{\kappa} \right). \quad (41)$$

C.2. One-step correction

As explained in Appendix B, the one-step correction removes the first-order bias from the plug-in estimator by adding the empirical mean of the efficient influence function evaluated at the empirical distribution $\hat{\mathbb{P}}$. In our setting, the resulting estimator becomes

$$\mathcal{L}^{\text{orth}}(g, \hat{\eta}) = \mathcal{L}^{\text{soft}}(g, \hat{\eta}) + \mathbb{P}_n \left[\mathbb{IF}_{\mathcal{L}^{\text{soft}}}(W, \hat{\mathbb{P}}) \right] \quad (42)$$

$$= \mathcal{L}^{\text{soft}}(g, \hat{\eta}) + \frac{1}{n} \sum_{i=1}^n \mathbb{IF}_{\mathcal{L}^{\text{soft}}}(w_i, \hat{\mathbb{P}}). \quad (43)$$

Since the influence function is evaluated at the empirical distribution $\hat{\mathbb{P}}$, all expectations are taken under $\hat{\mathbb{P}}$. Concretely, for any fixed x_i , we have

$$\hat{\mathbb{E}}_{X'}[C(x_i, X')] = \frac{1}{n} \sum_{j=1}^n C(x_i, x_j), \quad (44)$$

and, for the double expectation, we have

$$\hat{\mathbb{E}}_{X, X'}[\ell(X, X')] = \frac{1}{n^2} \sum_{j=1}^n \sum_{k=1}^n \ell(x_j, x_k). \quad (45)$$

We can now show that the empirical mean of the remainder term $B(W, \hat{\mathbb{P}})$ vanishes. Evaluating all expectations under the empirical distribution $\hat{\mathbb{P}}$, we have

$$\mathbb{P}_n[B(W, \hat{\mathbb{P}})] = \frac{1}{n} \sum_{i=1}^n \left\{ \hat{\mathbb{E}}_{X'}[\ell(x_i, X')] - \hat{\mathbb{E}}_{X, X'}[\ell(X, X')] + \hat{\mathbb{E}}_X[\ell(X, x_i)] - \hat{\mathbb{E}}_{X, X'}[\ell(X, X')] \right\} \quad (46)$$

$$= \frac{1}{n} \sum_{i=1}^n \left\{ \frac{1}{n} \sum_{j=1}^n \ell(x_i, x_j) - \frac{1}{n^2} \sum_{j=1}^n \sum_{k=1}^n \ell(x_j, x_k) + \frac{1}{n} \sum_{j=1}^n \ell(x_j, x_i) - \frac{1}{n^2} \sum_{j=1}^n \sum_{k=1}^n \ell(x_j, x_k) \right\} \quad (47)$$

$$= 0, \quad (48)$$

where the last equality follows by relabeling indices in the double sums.

Now consider the empirical mean of the $A(W, \hat{\mathbb{P}})$ term:

$$\mathbb{P}_n \left[\mathbb{IF}_{\mathcal{L}^{\text{soft}}}(W, \hat{\mathbb{P}}) \right] = \mathbb{P}_n \left[A(W, \hat{\mathbb{P}}) \right] \quad (49)$$

$$= \frac{1}{n} \sum_{i=1}^n \hat{\mathbb{E}}_{X'}[C(x_i, X')] (\phi_{\hat{\eta}}(w_i) - \hat{\tau}(x_i)) - \frac{1}{n} \sum_{i=1}^n \hat{\mathbb{E}}_X[C(X, x_i)] (\phi_{\hat{\eta}}(w_i) - \hat{\tau}(x_i)) \quad (50)$$

$$= \frac{1}{n^2} \sum_{i=1}^n \sum_{j=1}^n C(x_i, x_j) \left((\phi_{\hat{\eta}}(w_i) - \hat{\tau}(x_i)) - (\phi_{\hat{\eta}}(w_j) - \hat{\tau}(x_j)) \right), \quad (51)$$

where the last equality again follows by relabeling indices. Combining the plug-in loss with the one-step correction gives the empirical loss

$$\mathcal{L}^{\text{orth}}(g, \hat{\eta}) = \mathcal{L}^{\text{soft}}(g, \hat{\eta}) + \mathbb{P}_n \left[\mathbb{IF}_{\mathcal{L}^{\text{soft}}}(W, \hat{\mathbb{P}}) \right] \quad (52)$$

$$= \frac{1}{n^2} \sum_{i=1}^n \sum_{j=1}^n \left\{ -t_{\hat{\tau}}(x_i, x_j) \log p_g(x_i, x_j) - (1 - t_{\hat{\tau}}(x_i, x_j)) \log (1 - p_g(x_i, x_j)) \right\} \quad (53)$$

$$+ C(x_i, x_j) \left((\phi_{\hat{\eta}}(w_i) - \hat{\tau}(x_i)) - (\phi_{\hat{\eta}}(w_j) - \hat{\tau}(x_j)) \right) \}. \quad (54)$$

Recall that the correction weight satisfies

$$C(x_i, x_j) = \log \left(\frac{1 - p_g(x_i, x_j)}{p_g(x_i, x_j)} \right) \left(\frac{t_{\hat{\tau}}(x_i, x_j)(1 - t_{\hat{\tau}}(x_i, x_j))}{\kappa} \right), \quad (55)$$

where the first factor is exactly the derivative of the binary cross-entropy loss with respect to its label

$$\frac{\partial}{\partial t} \left(-t \log p - (1-t) \log(1-p) \right) = \log \left(\frac{1-p}{p} \right). \quad (56)$$

Since binary cross-entropy is affine in the label t , multiplying this derivative by any quantity can be absorbed into the label itself. Therefore, the entire correction is equivalent to using standard binary cross-entropy loss with pseudo labels

$$\tilde{t}_{\hat{\eta}}(w_i, w_j) = t_{\hat{\tau}}(x_i, x_j) + \frac{t_{\hat{\tau}}(x_i, x_j)(1 - t_{\hat{\tau}}(x_i, x_j))}{\kappa} \left((\phi_{\hat{\eta}}(w_i) - \hat{\tau}(x_i)) - (\phi_{\hat{\eta}}(w_j) - \hat{\tau}(x_j)) \right), \quad (57)$$

so that

$$\mathcal{L}^{\text{orth}}(g, \hat{\eta}) = \frac{1}{n^2} \sum_{i=1}^n \sum_{j=1}^n \left(-\tilde{t}_{\hat{\eta}}(w_i, w_j) \log p_g(x_i, x_j) - (1 - \tilde{t}_{\hat{\eta}}(w_i, w_j)) \log (1 - p_g(x_i, x_j)) \right). \quad (58)$$

C.3. Population loss and pseudo labels

At the population level, the derived loss can be written as binary cross-entropy between the model predictions and the pseudo labels

$$\mathcal{L}^{\text{orth}}(g, \eta) = \mathbb{E}_{W, W'} \left[-\tilde{t}_{\eta}(W, W') \log p_g(X, X') - (1 - \tilde{t}_{\eta}(W, W')) \log (1 - p_g(X, X')) \right], \quad (59)$$

with

$$\tilde{t}_{\eta}(W, W') = t_{\tau}(X, X') + \frac{t_{\tau}(X, X')(1 - t_{\tau}(X, X'))}{\kappa} \left((\phi_{\eta}(W) - \tau(X)) - (\phi_{\eta}(W') - \tau(X')) \right). \quad (60)$$

C.4. Proof of Neyman-orthogonality

Proof of Theorem 5.1. Let $\eta^0 = (\mu_1^0, \mu_0^0, e^0)$ denote the true nuisance components, and let g^0 be a population minimizer of the loss $\mathcal{L}^{\text{orth}}(g, \eta^0)$. Neyman-orthogonality requires that for any perturbation direction Δg and $\Delta \eta$,

$$D_{\eta} D_g \mathcal{L}^{\text{orth}}(g^0, \eta^0)[\Delta g, \Delta \eta] = 0. \quad (61)$$

We verify this condition by explicitly computing the cross-derivative evaluated at (g^0, η^0) and showing that it equals zero for each nuisance component, following the approach of [Morzywolek et al. \(2024\)](#).

Directional derivative with respect to g . We first write the loss in binary cross-entropy form

$$\mathcal{L}^{\text{orth}}(g, \eta) = \mathbb{E}_{W, W'} [\ell_{g, \eta}(W, W')] \quad (62)$$

$$= \mathbb{E}_{W, W'} \left[-\tilde{t}_{\eta}(W, W') \log p_g(X, X') - (1 - \tilde{t}_{\eta}(W, W')) \log (1 - p_g(X, X')) \right], \quad (63)$$

where $p_g(X, X') = \sigma(g(X) - g(X'))$ and $\tilde{t}_{\eta}(W, W')$ are the pseudo labels defined in Eq. (60).

To compute the directional derivative with respect to g , we consider the perturbation path

$$g_t(x) = g^0(x) + t \Delta g(x), \quad \text{with} \quad \Delta g(x) = g(x) - g^0(x), \quad (64)$$

such that, under mild regularity conditions,

$$D_g \mathcal{L}^{\text{orth}}(g^0, \eta)[\Delta g] = \frac{d}{dt} \mathcal{L}^{\text{orth}}(g_t, \eta) \Big|_{t=0} = \mathbb{E}_{W, W'} \left[\frac{d}{dt} \ell_{g_t, \eta}(W, W') \Big|_{t=0} \right]. \quad (65)$$

To evaluate the inner derivative, we apply the chain rule

$$\frac{d}{dt} \ell_{g_t, \eta}(W, W') \Big|_{t=0} = \frac{\partial \ell_{g_t, \eta}(W, W')}{\partial p_{g_t}(X, X')} \Big|_{t=0} \frac{\partial p_{g_t}(X, X')}{\partial (g_t(X) - g_t(X'))} \Big|_{t=0} \frac{\partial (g_t(X) - g_t(X'))}{\partial t} \Big|_{t=0} \quad (66)$$

$$= \frac{p_{g^0}(X, X') - \tilde{t}_\eta(W, W')}{p_{g^0}(X, X')(1 - p_{g^0}(X, X'))} p_{g^0}(X, X') (1 - p_{g^0}(X, X')) (\Delta g(X) - \Delta g(X')) \quad (67)$$

$$= (p_{g^0}(X, X') - \tilde{t}_\eta(W, W')) (\Delta g(X) - \Delta g(X')), \quad (68)$$

which leads to the result

$$D_g \mathcal{L}^{\text{orth}}(g^0, \eta)[\Delta g] = \mathbb{E} \left[(p_{g^0}(X, X') - \tilde{t}_\eta(W, W')) (\Delta g(X) - \Delta g(X')) \right]. \quad (69)$$

Orthogonality with respect to μ_1 . We now consider perturbations of the nuisance component μ_1 along the path

$$\mu_{1,s}(x) = \mu_1^0(x) + s \Delta \mu_1(x), \quad \text{with } \Delta \mu_1(x) = \mu_1(x) - \mu_1^0(x), \quad (70)$$

and write $\eta_s = (\mu_{1,s}, \mu_0^0, e^0)$ such that the directional derivative of interest becomes

$$D_{\mu_1} D_g \mathcal{L}^{\text{orth}}(g^0, \eta^0)[\Delta g, \Delta \mu_1] = \frac{d}{ds} D_g \mathcal{L}^{\text{orth}}(g^0, \eta_s)[\Delta g] \Big|_{s=0}, \quad (71)$$

and, under mild regularity conditions,

$$D_{\mu_1} D_g \mathcal{L}^{\text{orth}}(g^0, \eta^0)[\Delta g, \Delta \mu_1] = \frac{d}{ds} \mathbb{E} \left[(p_{g^0}(X, X') - \tilde{t}_{\eta_s}(W, W')) (\Delta g(X) - \Delta g(X')) \right] \Big|_{s=0} \quad (72)$$

$$= -\mathbb{E} \left[\frac{d}{ds} \tilde{t}_{\eta_s}(W, W') \Big|_{s=0} (\Delta g(X) - \Delta g(X')) \right]. \quad (73)$$

In order to evaluate the inner derivative, we substitute the definition of $\tilde{t}_{\eta_s}(W, W')$ from Equation (60), which yields

$$\begin{aligned} \frac{d}{ds} \tilde{t}_{\eta_s}(W, W') \Big|_{s=0} &= \frac{d}{ds} t_{\tau_s}(X, X') \Big|_{s=0} \\ &+ \frac{d}{ds} \underbrace{\frac{t_{\tau_s}(X, X')(1 - t_{\tau_s}(X, X'))}{\kappa}}_{A(s)} \underbrace{\left((\phi_{\eta_s}(W) - \tau_s(X)) - (\phi_{\eta_s}(W') - \tau_s(X')) \right)}_{B(s)} \Big|_{s=0}. \end{aligned} \quad (74)$$

For the first term, recall that

$$t_{\tau_s}(X, X') = \sigma \left(\frac{\tau_s(X) - \tau_s(X')}{\kappa} \right), \quad \text{with } \tau_s(X) = \mu_{1,s}(X) - \mu_0^0(X). \quad (75)$$

By applying the chain rule, we have

$$\frac{d}{ds} t_{\tau_s}(X, X') \Big|_{s=0} = \frac{t_{\tau^0}(X, X')(1 - t_{\tau^0}(X, X'))}{\kappa} (\Delta \mu_1(X) - \Delta \mu_1(X')). \quad (76)$$

For the second term, we apply the product rule, and for brevity write $\frac{d}{ds} A(s) \Big|_{s=0} = A'(0)$, such that

$$\frac{d}{ds} A(s) B(s) \Big|_{s=0} = A'(0) B(0) + A(0) B'(0) \quad (77)$$

$$\begin{aligned} &= A'(0) \left((\phi_{\eta^0}(W) - \tau^0(X)) - (\phi_{\eta^0}(W') - \tau^0(X')) \right) \\ &+ A(0) \frac{d}{ds} \left((\phi_{\eta_s}(W) - \tau_s(X)) - (\phi_{\eta_s}(W') - \tau_s(X')) \right) \Big|_{s=0}. \end{aligned} \quad (78)$$

Now, we can substitute the definition of $\phi_{\eta_s}(W)$ from Equation (29) to see that

$$\frac{d}{ds} (\phi_{\eta_s}(W) - \tau_s(X)) \Big|_{s=0} = \frac{d}{ds} \phi_{\eta_s}(W) \Big|_{s=0} - \frac{d}{ds} \tau_s(X) \Big|_{s=0} \quad (79)$$

$$= \frac{d}{ds} \left(\mu_{1,s}(X) - \mu_0^0(X) + \frac{T}{e^0(X)} (Y - \mu_{1,s}(X)) - \frac{1-T}{1-e^0(X)} (Y - \mu_0^0(X)) \right) \Big|_{s=0} - \Delta\mu_1(X) \quad (80)$$

$$= -\frac{T}{e^0(X)} \Delta\mu_1(X). \quad (81)$$

Therefore, the entire second term becomes

$$\begin{aligned} \frac{d}{ds} A(s)B(s) \Big|_{s=0} &= A'(0) \left((\phi_{\eta^0}(W) - \tau^0(X)) - (\phi_{\eta^0}(W') - \tau^0(X')) \right) \\ &\quad + \frac{t_{\tau^0}(X, X') (1 - t_{\tau^0}(X, X'))}{\kappa} \left(\frac{T'}{e^0(X')} \Delta\mu_1(X') - \frac{T}{e^0(X)} \Delta\mu_1(X) \right). \end{aligned} \quad (82)$$

Given the expressions for the derivatives of the soft label from Eq. (76) and the correction term from Eq. (82), we obtain

$$\begin{aligned} \frac{d}{ds} \tilde{t}_{\eta_s}(W, W') \Big|_{s=0} &= A'(0) \left((\phi_{\eta^0}(W) - \tau^0(X)) - (\phi_{\eta^0}(W') - \tau^0(X')) \right) \\ &\quad + \frac{t_{\tau^0}(X, X') (1 - t_{\tau^0}(X, X'))}{\kappa} \left(\left(1 - \frac{T}{e^0(X)}\right) \Delta\mu_1(X) - \left(1 - \frac{T'}{e^0(X')}\right) \Delta\mu_1(X') \right). \end{aligned} \quad (83)$$

Finally, we can consider the directional derivative of interest in Eq. (73), and apply iterated expectations to yield

$$D_{\mu_1} D_g \mathcal{L}^{\text{orth}}(g^0, \eta^0)[\Delta g, \Delta\mu_1] = -\mathbb{E}_{W, W'} \left[\frac{d}{ds} \tilde{t}_{\eta_s}(W, W') \Big|_{s=0} (\Delta g(X) - \Delta g(X')) \right] \quad (84)$$

$$= -\mathbb{E}_{X, X'} \left[\mathbb{E}_{T, T', Y, Y' | X, X'} \left[\frac{d}{ds} \tilde{t}_{\eta_s}(W, W') \Big|_{s=0} \right] (\Delta g(X) - \Delta g(X')) \right] \quad (85)$$

$$= 0, \quad (86)$$

where the last equality follows from

$$\mathbb{E}_{T, Y | X} \left[1 - \frac{T}{e^0(X)} \right] = 0, \quad \text{and} \quad \mathbb{E}_{T, Y | X} \left[\phi_{\eta^0}(W) - \tau^0(X) \right] = 0, \quad (87)$$

and likewise for the primed counterparts.

This shows that for any perturbation directions Δg and $\Delta\mu_1$,

$$D_{\mu_1} D_g \mathcal{L}^{\text{orth}}(g^0, \eta^0)[\Delta g, \Delta\mu_1] = 0. \quad (88)$$

and therefore establishes that the loss $\mathcal{L}^{\text{orth}}$ is Neyman-orthogonal with respect to the nuisance component μ_1 .

Orthogonality with respect to μ_0 . For the nuisance component μ_0 , the proof is analogous to the case of μ_1 with some minor differences. We consider perturbations along the path

$$\mu_{0,s}(x) = \mu_0^0(x) + s \Delta\mu_0(x), \quad \text{with} \quad \Delta\mu_0(x) = \mu_0(x) - \mu_0^0(x), \quad (89)$$

and write $\eta_s = (\mu_1^0, \mu_{0,s}, e^0)$. The directional derivative of interest is then

$$D_{\mu_0} D_g \mathcal{L}^{\text{orth}}(g^0, \eta^0)[\Delta g, \Delta\mu_0] = \frac{d}{ds} D_g \mathcal{L}^{\text{orth}}(g^0, \eta_s)[\Delta g] \Big|_{s=0} \quad (90)$$

$$= -\mathbb{E} \left[\frac{d}{ds} \tilde{t}_{\eta_s}(W, W') \Big|_{s=0} (\Delta g(X) - \Delta g(X')) \right]. \quad (91)$$

By the same steps as in the case of μ_1 , but using that $\tau_s(x) = \mu_1^0(x) - \mu_{0,s}(x)$, we get

$$\begin{aligned} \frac{d}{ds} \tilde{t}_{\eta_s}(W, W') \Big|_{s=0} &= \frac{t_{\tau^0}(X, X')(1 - t_{\tau^0}(X, X'))}{\kappa} \left(\left(\frac{1 - T}{1 - e^0(X)} - 1 \right) \Delta\mu_0(X) - \left(\frac{1 - T'}{1 - e^0(X')} - 1 \right) \Delta\mu_0(X') \right) \\ &+ \frac{d}{ds} \left(\frac{t_{\tau_s}(X, X')(1 - t_{\tau_s}(X, X'))}{\kappa} \right) \Big|_{s=0} \left((\phi_{\eta^0}(W) - \tau^0(X)) - (\phi_{\eta^0}(W') - \tau^0(X')) \right). \end{aligned} \quad (92)$$

We can then express the directional derivative using iterated expectations as

$$D_{\mu_0} D_g \mathcal{L}^{\text{orth}}(g^0, \eta^0)[\Delta g, \Delta\mu_0] = -\mathbb{E}_{X, X'} \left[\mathbb{E}_{T, T', Y, Y' | X, X'} \left[\frac{d}{ds} \tilde{t}_{\eta_s}(W, W') \Big|_{s=0} \right] (\Delta g(X) - \Delta g(X')) \right] \quad (93)$$

$$= 0, \quad (94)$$

since

$$\mathbb{E}_{T, Y | X} \left[\frac{1 - T}{1 - e^0(X)} - 1 \right] = 0, \quad \text{and} \quad \mathbb{E}_{T, Y | X} \left[\phi_{\eta^0}(W) - \tau^0(X) \right] = 0, \quad (95)$$

and likewise for the primed counterparts. This derivation establishes orthogonality of $\mathcal{L}^{\text{orth}}$ with respect to the nuisance component μ_0 .

Orthogonality with respect to e .

For the propensity score e , the orthogonality argument follows the same overall strategy as for μ_1 and μ_0 , but the dependence of \tilde{t}_η on e enters only through the doubly robust score ϕ_η (Eq. (29)). We consider perturbations of e along the path

$$e_s(x) = e^0(x) + s \Delta e(x), \quad \text{with} \quad \Delta e(x) = e(x) - e^0(x), \quad (96)$$

and define $\eta_s = (\mu_1^0, \mu_0^0, e_s)$. The directional derivative of interest is then

$$D_e D_g \mathcal{L}^{\text{orth}}(g^0, \eta^0)[\Delta g, \Delta e] = \frac{d}{ds} D_g \mathcal{L}^{\text{orth}}(g^0, \eta_s)[\Delta g] \Big|_{s=0} \quad (97)$$

$$= -\mathbb{E} \left[\frac{d}{ds} \tilde{t}_{\eta_s}(W, W') \Big|_{s=0} (\Delta g(X) - \Delta g(X')) \right]. \quad (98)$$

Now, by relying on the definition of $\tilde{t}_{\eta_s}(W, W')$ from Equation (60), the inner derivative simplifies to

$$\frac{d}{ds} \tilde{t}_{\eta_s}(W, W') \Big|_{s=0} = \frac{t_{\tau^0}(X, X')(1 - t_{\tau^0}(X, X'))}{\kappa} \cdot \frac{d}{ds} \left((\phi_{\eta_s}(W) - \tau^0(X)) - (\phi_{\eta_s}(W') - \tau^0(X')) \right) \Big|_{s=0} \quad (99)$$

$$= \frac{t_{\tau^0}(X, X')(1 - t_{\tau^0}(X, X'))}{\kappa} \left(\frac{d}{ds} \phi_{\eta_s}(W) \Big|_{s=0} - \frac{d}{ds} \phi_{\eta_s}(W') \Big|_{s=0} \right), \quad (100)$$

since only the doubly robust score ϕ_{η_s} depends on s .

If we now focus on the derivative of this doubly robust score, we get

$$\frac{d}{ds} \phi_{\eta_s}(W) \Big|_{s=0} = \frac{d}{ds} \left(\mu_1^0(X) - \mu_0^0(X) + \frac{T}{e^0(X)} (Y - \mu_1^0(X)) - \frac{1 - T}{1 - e^0(X)} (Y - \mu_0^0(X)) \right) \Big|_{s=0} \quad (101)$$

$$= -T(Y - \mu_1^0(X)) \frac{\Delta e(X)}{e^0(X)^2} - (1 - T)(Y - \mu_0^0(X)) \frac{\Delta e(X)}{(1 - e^0(X))^2} \quad (102)$$

$$= -\Delta e(X) \left(\frac{T(Y - \mu_1^0(X))}{e^0(X)^2} + \frac{(1 - T)(Y - \mu_0^0(X))}{(1 - e^0(X))^2} \right). \quad (103)$$

We can again express the directional derivative using iterated expectations as

$$D_e D_g \mathcal{L}^{\text{orth}}(g^0, \eta^0)[\Delta g, \Delta e] = -\mathbb{E}_{X, X'} \left[\mathbb{E}_{T, T', Y, Y' | X, X'} \left[\frac{d}{ds} \tilde{t}_{\eta_s}(W, W') \Big|_{s=0} \right] (\Delta g(X) - \Delta g(X')) \right] \quad (104)$$

$$= 0, \quad (105)$$

where the last equality follows from

$$\mathbb{E}_{T, T', Y, Y' | X, X'} \left[\frac{T(Y - \mu_1^0(X))}{e^0(X)^2} + \frac{(1 - T)(Y - \mu_0^0(X))}{(1 - e^0(X))^2} \right] \quad (106)$$

$$= \frac{1}{e^0(X)^2} \mathbb{E}_{T, Y | X} [T(Y - \mu_1^0(X))] + \frac{1}{(1 - e^0(X))^2} \mathbb{E}_{T, Y | X} [(1 - T)(Y - \mu_0^0(X))] \quad (107)$$

$$= 0, \quad (108)$$

and likewise for the corresponding primed term, which therefore establishes that $\mathcal{L}^{\text{orth}}$ is Neyman-orthogonal with respect to e .

Conclusion. We have shown that for each nuisance component $\eta = (\mu_1, \mu_0, e)$ and for arbitrary perturbation directions $(\Delta g, \Delta \eta)$, the cross-derivative of the loss satisfies

$$D_{\mu_1} D_g \mathcal{L}^{\text{orth}}(g^0, \eta^0)[\Delta g, \Delta \mu_1] = D_{\mu_0} D_g \mathcal{L}^{\text{orth}}(g^0, \eta^0)[\Delta g, \Delta \mu_0] = D_e D_g \mathcal{L}^{\text{orth}}(g^0, \eta^0)[\Delta g, \Delta e] = 0. \quad (109)$$

Therefore, the loss $\mathcal{L}^{\text{orth}}$ is Neyman-orthogonal with respect to the nuisance components (μ_1, μ_0, e) . \square

D. Population optima of the considered learning objectives

In this section, we characterize the population optima of our considered losses at the true nuisances η^0 . We show that all losses aim to recover a scoring function $g(x)$ whose ranking matches that of the conditional average treatment effect $\tau(x)$, but they differ in how strongly they constrain g . Therefore, every population-optimal solution must preserve the τ -induced ordering, and the losses only differ in how much additional structure they impose on $g(x)$. We then discuss the role of the smoothing parameter κ in the orthogonal ranking loss $\mathcal{L}^{\text{orth}}$.

D.1. Population optima

Minimizer of the mean squared error loss. The simplest objective that we consider is the mean squared error between the scoring function $g(x)$ and the true CATE $\tau^0(x)$. It is given by

$$\mathcal{L}^{\text{cate}}(g, \eta^0) = \mathbb{E}_X \left[(g(X) - \tau^0(X))^2 \right], \quad (110)$$

and is uniquely minimized at $g^0(x) = \tau^0(x)$. Therefore, the minimizer preserves the τ -induced ordering as it fully identifies the CATE. Minimizing this loss requires recovering the full structure of $\tau(x)$ and not just the ranking.

Population optima of the binary ranking loss. We next consider the binary ranking loss, which is binary cross-entropy between the pairwise probability predictions of the model $p_g(x, x')$ and the binary indicators of the τ -induced ordering. It is given by

$$\mathcal{L}^{\text{bin}}(g, \eta^0) = \mathbb{E}_{X, X'} \left[-b_{\tau^0}(X, X') \log p_g(X, X') - (1 - b_{\tau^0}(X, X')) \log (1 - p_g(X, X')) \right], \quad (111)$$

where

$$p_g(X, X') = \sigma(g(X) - g(X')), \quad \text{and} \quad b_{\tau^0}(X, X') = \mathbf{I}\{\tau^0(X) > \tau^0(X')\}. \quad (112)$$

If we consider a given pair (x, x') , the infimum of the loss contribution equals zero and is approached when the model probability $p_g(x, x')$ converges to the binary label $b_{\tau^0}(x, x')$. This occurs as the margin $g(x) - g(x')$ tends to $+\infty$ if $b_{\tau^0}(x, x') = 1$ and to $-\infty$ otherwise. For any finite model g , the infimum cannot be attained, but correctly ordered pairs can have a loss contribution arbitrarily close to zero. In contrast, if a candidate model g misorders a pair, the margin $g(x) - g(x')$ will have the wrong sign, and the loss contribution remains strictly bounded away from zero with a positive constant. Therefore, if g does not follow the τ -induced ordering, there must be at least one such misordered pair keeping the population loss bounded away from its infimum. If g does respect the τ -induced ordering, all pairwise loss contributions can be made arbitrarily small by scaling g . It follows that any population-optimal solution of \mathcal{L}^{bin} , in the sense of achieving a risk arbitrarily close to the infimum, must preserve the ordering of the treatment effects.

The binary ranking loss does not admit a unique population minimizer, as its infimum cannot be attained by a finite model g . Once the model g agrees with the ordering induced by τ , scaling g by any positive constant increases all pairwise margins and drives the loss arbitrarily close to zero. Additionally, as the loss depends only on the difference $g(x) - g(x')$, adding a constant shift to g leaves all pairwise predictions $p_g(x, x')$, and thus the total loss, unchanged. As a result, any scoring function g that follows the τ -ordering can be considered population-optimal. These are all functions of the form $g^0(x) = h(\tau^0(x))$ for some strictly increasing transformation h . This invariance is precisely why learning a ranking of treatment effects is an easier problem than learning the precise treatment effect magnitudes.

Minimizers of the soft ranking loss. We now consider the soft ranking loss, which is binary cross-entropy between the pairwise probability predictions of the model $p_g(x, x')$ and smoothed pairwise targets based on the CATE differences. The loss is given by

$$\mathcal{L}^{\text{soft}}(g, \eta^0) = \mathbb{E}_{X, X' \sim \mathbb{P}(X)} \left[-t_{\tau^0}(X, X') \log p_g(X, X') - (1 - t_{\tau^0}(X, X')) \log (1 - p_g(X, X')) \right], \quad (113)$$

where

$$p_g(X, X') = \sigma(g(X) - g(X')), \quad \text{and} \quad t_{\tau^0}(X, X') = \sigma\left(\frac{\tau^0(X) - \tau^0(X')}{\kappa}\right), \quad (114)$$

with $\kappa > 0$ a smoothing parameter.

Unlike the binary ranking targets, the soft targets $t_{\tau^0}(x, x')$ do not only encode the ordering of $\tau^0(x) - \tau^0(x')$, but also the magnitude of this difference, scaled by $(1/\kappa)$. The loss contribution for a pair (x, x') is exactly minimized when the model probability $p_g(x, x')$ matches the soft targets $t_{\tau^0}(x, x')$, which occurs precisely when

$$g(x) - g(x') = \frac{\tau^0(x) - \tau^0(x')}{\kappa}. \quad (115)$$

This constraint is satisfied jointly for all pairs when the scoring model takes the form

$$g^0(x) = \frac{1}{\kappa} \tau^0(x) + c, \quad (116)$$

for some constant $c \in \mathbb{R}$. In contrast to the binary ranking loss, the soft ranking loss identifies $\tau(x)$ up to an additive constant and a fixed scaling factor $(1/\kappa)$, imposing more structure on g than just the ranking.

Minimizers of the orthogonal loss. We finally consider the orthogonal ranking loss, which was derived based on the influence function of the soft ranking loss. The population objective is given by

$$\mathcal{L}^{\text{orth}}(g, \eta^0) = \mathbb{E}_{W, W'} \left[-\tilde{t}_{\eta^0}(W, W') \log p_g(X, X') - (1 - \tilde{t}_{\eta^0}(W, W')) \log (1 - p_g(X, X')) \right], \quad (117)$$

where $p_g(X, X') = \sigma(g(X) - g(X'))$, and where the pseudo labels are defined as

$$\tilde{t}_{\eta^0}(W, W') = t_{\tau^0}(X, X') + \frac{t_{\tau^0}(X, X') (1 - t_{\tau^0}(X, X'))}{\kappa} \left((\phi_{\eta^0}(W) - \tau^0(X)) - (\phi_{\eta^0}(W') - \tau^0(X')) \right). \quad (118)$$

Since the orthogonal loss is also a binary cross-entropy objective, the loss contribution of a pair (x, x') is minimized when the model probability $p_g(x, x')$ matches the conditional expectation of the pseudo labels given $X = x$ and $X = x'$, or

$$p_g(x, x') = \mathbb{E}[\tilde{t}_{\eta^0}(W, W') \mid X = x, X' = x']. \quad (119)$$

To evaluate this expectation, we can rely on the property of the doubly robust score, i.e.,

$$\mathbb{E}[\phi_{\eta^0}(W) - \tau^0(X) \mid X] = 0, \quad (120)$$

and likewise for the primed counterpart, which implies that the correction term in $\tilde{t}_{\eta^0}(W, W')$ has zero conditional mean. Consequently, the loss contribution is minimized when

$$p_g(x, x') = \mathbb{E}[\tilde{t}_{\eta^0}(W, W') \mid X = x, X' = x'] = t_{\tau^0}(x, x'). \quad (121)$$

This means that the correction based on the influence function does not change the population minimizers, and the orthogonal loss has the same minimizers as the soft ranking loss

$$g^0(x) = \frac{1}{\kappa} \tau^0(x) + c. \quad (122)$$

D.2. Interpretation of the smoothness parameter κ

Now that we have derived the population optima of the considered loss functions, we discuss the behavior of the orthogonal ranking loss as a function of the smoothness parameter κ . While, for any fixed and finite $\kappa > 0$, the population minimizers preserve the ordering of the treatment effects, the choice of κ strongly influences the shape of the loss landscape and the structure imposed on g .

Small κ . As $\kappa \rightarrow 0$, the soft targets converge to the targets of the binary ranking loss, we yield

$$t_{\tau^0}(X, X') = \sigma \left(\frac{\tau^0(X) - \tau^0(X')}{\kappa} \right) \longrightarrow b_{\tau^0}(X, X') = \mathbf{I}\{\tau^0(X) > \tau^0(X')\}. \quad (123)$$

Accordingly, both the soft and orthogonal ranking losses ($\mathcal{L}^{\text{soft}}$ and $\mathcal{L}^{\text{orth}}$) approach the binary ranking loss (\mathcal{L}^{bin}). At the same time, their population minimizers $g^0(x) = \tau^0(x)/\kappa + c$ become unbounded, reflecting that the binary ranking loss

does not admit a finite population minimizer. In this regime, any scoring function that preserves the ordering induced by $\tau^0(x)$ can achieve a population risk arbitrarily close to the infimum.

This behavior can also be understood through the geometry of these losses. At the population optimum, the second derivative of a single pairwise loss contribution (of both $\mathcal{L}^{\text{soft}}$ and $\mathcal{L}^{\text{orth}}$), with respect to the margin $g(x) - g(x')$, is given by

$$\nabla_{g(x)-g(x')}^2 \ell(g^0, \eta^0) = p_{g^0}(x, x') (1 - p_{g^0}(x, x')) \quad (124)$$

$$= \sigma \left(\frac{\tau^0(x) - \tau^0(x')}{\kappa} \right) \left(1 - \sigma \left(\frac{\tau^0(x) - \tau^0(x')}{\kappa} \right) \right). \quad (125)$$

As the smoothing parameter κ goes to zero, the loss becomes locally flat along directions that preserve the τ -induced ordering. In the limit, the learning problem therefore reduces to recovering the ranking of the treatment effects, rather than the exact magnitudes of their differences.

Intermediate κ . For $\kappa = 1$, the soft targets become $t_{\tau^0}(X, X') = \sigma(\tau^0(X) - \tau^0(X'))$, and encode both the ordering and the relative magnitude of the treatment effect differences. The population minimizer of the soft and orthogonal ranking losses then takes the form $g^0(x) = \tau^0(x) + c$, implying that the learning problem requires recovering the full functional form of $\tau^0(x)$, rather than only the ordering. This behavior is also reflected in the curvature of the loss around the optimum (Eq. (125)) which is now strictly positive at the population minimizer and penalizes deviations of the margins $g(x) - g(x')$ from $\tau^0(x) - \tau^0(x')$. This choice of parameter κ therefore enforces the most structure on the scoring function g .

Large κ . As $\kappa \rightarrow \infty$, the soft targets satisfy

$$t_{\tau^0}(X, X') = \sigma \left(\frac{\tau^0(X) - \tau^0(X')}{\kappa} \right) \rightarrow \frac{1}{2}, \quad (126)$$

and therefore become independent of the ordering and the magnitude of the treatment effect differences. Consequently, the population minimizer of the soft and orthogonal losses becomes $g^0(x) = c$, with the model predictions collapsing to $p_{g^0}(x, x') = 1/2$. In this regime, where $\kappa \rightarrow \infty$, all ordering information is lost, which enforces a constant scoring function $g(x)$. This arises only in the limit, and for any fixed and finite $\kappa > 0$, both the soft and orthogonal targets remain dependent on $\tau^0(x) - \tau^0(x')$ and therefore preserve the ordering of treatment effects.

Choice of κ . Since our objective is purely ranking of treatment effects, the discussion above suggests choosing κ to be small. At the population level, this reduces the learning problem to recovering only the τ -induced ordering. In practice however, the pairwise targets $t_{\tau^0}(x, x')$ or $b_{\tau^0}(x, x')$ are not observed and must be estimated from data. Such estimates can introduce plug-in bias, which is precisely the issue addressed by the orthogonal loss $\mathcal{L}^{\text{orth}}$.

At the same time, as κ decreases, the orthogonal correction amplifies for pairs with similar treatment effects, which increases the variability of $\tilde{t}_\eta(w, w')$ in finite samples. Consequently, while smaller values of κ impose weaker structural constraints on g and move the problem closer to pure ranking, they also amplify the estimation noise in finite samples. The choice of κ thus reflects a bias-variance trade-off. We propose to select κ using an approximation of the AUTOC criterion on a validation set, which aligns the model selection directly with the ranking objective (Chernozhukov et al., 2025).

E. Data-generating processes

This appendix provides additional information on the data-generating processes used in our experiments. We consider both a fully synthetic setting, where covariates are generated from known distributions, and semi-synthetic settings, where real-world covariates are combined with simulated treatments and outcomes. This allows us to evaluate *Rank-Learner* under controlled conditions and under realistic feature distributions. The full implementation of all data-generating processes and experiments are available on <https://anonymous.4open.science/r/rank-learner>.

E.1. Synthetic data-generating process

We begin our experiments on a fully synthetic dataset, which enables a controlled evaluation of the proposed *Rank-Learner* against pointwise CATE estimators and a non-orthogonal ranker under known ground-truth treatment effects. The data-generating process is adapted from prior work (Kamran et al., 2024) and is constructed such that the treatment effects are generated as a strictly increasing, non-linear transformation of a latent score $s(x)$. As a result, the ranking of treatment effects is fully determined by $s(x)$, while their exact magnitudes depend on the transformation, allowing us to decouple the ranking problem from pointwise effect estimation. The treatment assignment depends on $s(x)$ and an independent component (to induce confounding while maintaining overlap), and the baseline outcome $\mu_0(x)$ is generated primarily from covariates not used in $s(x)$, such that outcome prediction does not fully recover the treatment effect ranking.

The covariates $X \in \mathbb{R}^{10}$ are sampled i.i.d. from a multivariate standard normal distribution,

$$X \sim \mathcal{N}(0, I_{10}). \quad (127)$$

We define a latent score $s(X)$ that fully determines the ranking of treatment effects as

$$s(X) = 0.8X_1 + 0.6X_2 + 0.4X_3 + 0.3X_1^2 - 0.2X_2X_3. \quad (128)$$

The treatment effects are generated as strictly increasing, non-linear transformations of $s(X)$, i.e.,

$$\tau(X) = s(X) + 0.5 \tanh(s(X)). \quad (129)$$

The nuisance components (propensity score and potential outcomes) are generated as

$$e(X) = \sigma(0.8s(X) + 0.6(X_6 - 0.5X_7)), \quad (130)$$

$$\mu_0(X) = 0.5X_2 - 0.4X_3 + 0.3 \sin(X_4) + 0.2(X_5^2 - 1), \quad (131)$$

$$\mu_1(X) = \mu_0(X) + \tau(X) \quad (132)$$

where $\sigma(\cdot)$ denotes the logistic sigmoid.

The treatment indicators and observed outcomes are sampled as

$$T \sim \text{Bernoulli}(e(X)) \quad (133)$$

$$Y = T\mu_1(X) + (1 - T)\mu_0(X) + \varepsilon, \quad \varepsilon \sim \mathcal{N}(0, 0.6^2). \quad (134)$$

For all synthetic experiments, we generate a fixed test set of 1,000 samples that is exclusively used for evaluation. Training data are generated with varying sample sizes (ranging from 100 to 2,000 samples). This allows us to study the ranking performance as a function of training size, which directly affects the quality of the estimated nuisance components. For each considered training size n , we use sample splitting: n samples are used to estimate the nuisance components (of which 80% are used to fit the models and 20% for validation), and an independent set of n samples is used to train the second-stage models (pointwise CATE estimators or rankers; again split into 80% for training and 20% for validation). All experiments are repeated over five random seeds, which affect both data sampling and weight initialization of the models.

E.2. Semi-synthetic data-generating processes

In the semi-synthetic setting, we use real-world covariates from three established datasets covering distinct application domains: MOVIELENS (recommender systems) (Harper & Konstan, 2015), MIMIC-III (healthcare) (Johnson et al., 2016), and the CURRENT POPULATION SURVEY (public policy) (Flood et al., 2025). This preserves realistic feature distributions while enabling a controlled evaluation with access to ground-truth treatment effects. The exact data-generating processes can be found in the accompanying code repository.

Across the three semi-synthetic datasets, we follow the same data-generating structure as in the fully synthetic setting. In particular, treatment effects are generated as strictly increasing, non-linear transformations of a latent score $s(x)$, such that the ranking of treatment effects is fully determined by $s(x)$, while the magnitudes depend on the transformation. Treatment assignment depends on $s(x)$ and an independent component, to induce confounding while maintaining overlap, and $\mu_0(x)$ is generated largely independently of $s(x)$. All components of the generated data are constructed with a realistic, domain-specific interpretation, such that treatment assignment, outcomes, and treatment effects reflect plausible mechanisms for the considered applications.

For all semi-synthetic experiments, we generate a fixed test set of 1,000 samples that is used exclusively for evaluation. As in the synthetic setting, we perform sample splitting with nuisance components and second-stage models trained on separate samples. We consider a fixed training size of 1,000 samples of which 80% is used to fit the models and 20% for validation. All experiments are repeated over five random seeds, which affect both data sampling and weight initialization of the models.

- **MOVIELENS** (Harper & Konstan, 2015). From this dataset, we extract user-level covariates capturing demographics (age, gender, and occupation), behavioral traits (mean and standard deviation of past movie ratings), and features capturing movie preference (genre-specific share of watched movies). We simulate a setting where the treatment corresponds to exposure to a targeted advertisement on a movie platform, and the outcome represents user engagement. Treatment assignment is biased towards specific occupational groups, in particular students, and the treatment effects are primarily driven by user preferences, reflecting that users whose preferred genres align more closely with the advertised content respond more positively. Baseline engagement is mostly driven by the historical rating behavior and is only weakly correlated with the treatment effects.

- **MIMIC-III** (Johnson et al., 2016). From this dataset, we extract patient-level covariates capturing demographics (age and gender) and vital sign measurements (heart rate, blood pressure, arterial pressure, respiratory rate, and oxygen saturation). We simulate a clinical decision-making setting in which a medical treatment is administered that affects patient recovery (the outcome reflects a continuous recovery score). The treatment effects are primarily driven by instability in blood circulation (based on abnormal blood pressure and arterial pressure measurements), reflecting that patients with a more severe condition can benefit most from treatment. Treatment assignment is biased towards patients exhibiting signs of acute physiological distress, such as an elevated heart rate and respiratory rate (while also depending on blood circulation to induce confounding). Baseline recovery is primarily driven by fever and oxygen saturation and is only mildly correlated with the treatment effects.

- **CPS** (Flood et al., 2025). From this dataset, we extract individual-level covariates capturing demographics (age, gender, and educational attainment), household structure (marital status and number of dependents), and labor-market characteristics (hours worked per week, weeks worked per year, firm size, wage, and household income). We simulate a policy intervention (representing, for instance, a job-training program), with the outcome representing a continuous measure of future earnings potential. Treatment effects are primarily driven by individual skill readiness and economic need (higher effects for younger individuals with a low current income and a high educational attainment). Treatment assignment follows a household-based eligibility heuristic that prioritizes individuals with dependents and greater family responsibilities. Baseline outcomes are driven mainly by employment intensity and current income and are moderately correlated with the treatment effects.

E.3. Implementation details

This section provides the implementation details shared between all experiments. The same model architectures and training procedures are used across model components and datasets. All experiments are conducted on a single machine equipped with an NVIDIA GeForce GTX 2080 GPU, and training is computationally lightweight, with most models converging within a few minutes. All models (nuisance components, CATE regressors, and rankers) are implemented as feedforward neural networks with a single hidden layer and ReLU activations. The output layers are linear for regression tasks and sigmoid for binary classification tasks. The models are trained using the Adam optimizer with a maximum of 50 epochs

and early stopping based on the validation loss, with a patience of five epochs. The model parameters with the lowest corresponding validation loss are retained.

Hyperparameters are minimally tuned once via a random search over a validation dataset (12 runs), and then fixed across all experiments and seeds. The tuned hyperparameters include the hidden layer width $\in \{64, 128\}$, learning rate $\in \{10^{-4}, 3 \cdot 10^{-4}, 5 \cdot 10^{-4}, 10^{-3}\}$, weight decay $\in \{0, 10^{-5}, 10^{-4}\}$, and batch size $\in \{128, 256\}$. For the *Rank-Learner* and the plug-in ranker, the smoothness parameter $\kappa \in \{0.25, 0.5, 1, 1.5, 3\}$, along with the other hyperparameters, are tuned based on the approximated validation AUTOC. In addition, since the orthogonal correction in the *Rank-Learner* pseudo labels can, in rare cases, yield values outside the $(0, 1)$ range, we clip these labels to $(0, 1)$ as a simple stabilization strategy.

F. Additional experimental results

In this section, we report the complete experimental results for the synthetic and semi-synthetic benchmarks, which extend the summarized findings presented in the main body. Next to AUTOC, we additionally report the *mean policy value* \bar{V} , which measures the mean outcome in the population under the implied policy that treats the top- k individuals ranked by \hat{g} , averaged over all k , on the test set.

F.1. Results across varying training sizes

Table 5 reports the ranking performance on the synthetic dataset across training sizes. Our proposed *Rank-Learner* consistently outperforms the non-orthogonal plug-in ranker and the pointwise CATE estimators, both on AUTOC and mean policy value, across sample sizes. The strong performance is most pronounced when nuisance estimation error is more difficult (i.e., in settings with smaller dataset sizes, which confirms our theory), where the *Rank-Learner* achieves the best ranking metrics and reduced variability across seeds. As n grows, the performance gaps between the methods gradually narrow and all methods converge towards the oracle values of the metrics. This observed convergence of the methods is expected and aligns with theory since the nuisance estimation quality improves with growing n , as reported in Table 6. As expected, when the estimation error in the nuisances is larger (i.e., in regimens with smaller sample sizes), the performance of plug-in methods drops in comparison to our proposed *Rank-Learner*. The orthogonal methods (i.e., *Rank-Learner* and DR-learner) are designed to be first-order insensitive to these estimation errors, which is reflected in their performance.

Table 5. Synthetic benchmark (main results): Test AUTOC and mean policy value (mean \pm std dev over five seeds) across training sizes. *Higher is better*. The oracle column reports the metrics obtained by ranking the test set using the true treatment effects. Best mean is shown in **bold**.

Metric	Method	$n = 100$	$n = 250$	$n = 500$	$n = 1,000$	$n = 2,000$	oracle
AUTOC (\uparrow)	T-learner	0.88 ± 0.17	0.96 ± 0.14	1.24 ± 0.05	1.32 ± 0.02	1.36 ± 0.00	
	DR-learner	0.80 ± 0.18	1.16 ± 0.12	1.28 ± 0.05	1.33 ± 0.02	1.36 ± 0.02	
	Plug-in ranker	0.69 ± 0.32	0.95 ± 0.14	1.24 ± 0.06	1.31 ± 0.02	1.36 ± 0.00	1.40
	Rank-learner (ours)	0.94 ± 0.21	1.28 ± 0.03	1.30 ± 0.03	1.34 ± 0.01	1.37 ± 0.00	
\bar{V} (\uparrow)	T-learner	0.46 ± 0.04	0.49 ± 0.03	0.56 ± 0.01	0.57 ± 0.01	0.58 ± 0.00	
	DR-learner	0.42 ± 0.05	0.53 ± 0.03	0.55 ± 0.02	0.57 ± 0.00	0.58 ± 0.00	
	Plug-in ranker	0.38 ± 0.09	0.48 ± 0.03	0.56 ± 0.01	0.57 ± 0.01	0.58 ± 0.00	0.59
	Rank-learner (ours)	0.46 ± 0.05	0.55 ± 0.01	0.56 ± 0.01	0.57 ± 0.00	0.58 ± 0.00	

Table 6. Synthetic benchmark (nuisance estimation): Nuisance estimation quality across training sizes, evaluated on the test set (mean \pm std dev over seeds). MSE denotes mean squared error and BCE denotes binary cross-entropy. *Lower is better*.

Metric	$n = 100$	$n = 250$	$n = 500$	$n = 1,000$	$n = 2,000$
MSE (μ_0)	0.30 ± 0.09	0.24 ± 0.06	0.14 ± 0.03	0.11 ± 0.04	0.08 ± 0.03
MSE (μ_1)	1.72 ± 0.28	1.66 ± 0.23	0.78 ± 0.22	0.35 ± 0.05	0.18 ± 0.03
BCE (e)	0.689 ± 0.004	0.685 ± 0.009	0.678 ± 0.011	0.667 ± 0.003	0.663 ± 0.002

F.2. Effect of pair subsampling

Figure 5 shows the effect of subsampling training pairs on the ranking performance of *Rank-Learner*. In this experiment, we fix the training size to $n = 1,000$ and estimate the nuisance components using sample-splitting. The second-stage ranker is then trained using only a fraction of the n^2 available training pairs, with fractions ranging from 0.01% to 50%. For each fraction, pairs are sampled randomly per epoch, and the results are averaged across five random seeds.

Despite the quadratic number of possible training pairs, *Rank-Learner* achieves strong ranking performance using only a small subset of the available training pairs. In particular, training on approximately 1% of the n^2 possible pairs is sufficient to recover most of the attainable AUTOC, with diminishing returns beyond this point. This indicates that the computational cost of pairwise training can be substantially reduced without sacrificing performance. This result, together with Table 6, suggests that the performance differences across training sizes ($n = 100$ to $n = 2,000$) are primarily driven by improvements in the nuisance estimates, rather than by the number of sampled training pairs.

Orthogonal Ranking of Treatment Effects

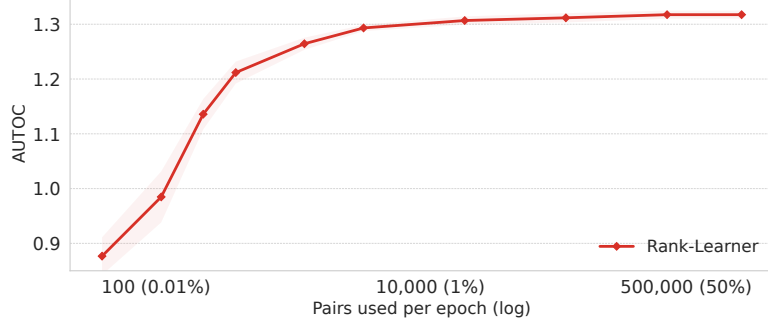


Figure 5. Synthetic benchmark (pair subsampling). Test AUTOOC (mean \pm s.e. over five seeds) of *Rank-Learner* as a function of the number of sampled training pairs per epoch ($n = 1,000$ with $n^2 = 10^6$ possible training pairs). *Higher is better*. The horizontal axis shows the fraction of pairs used (log).

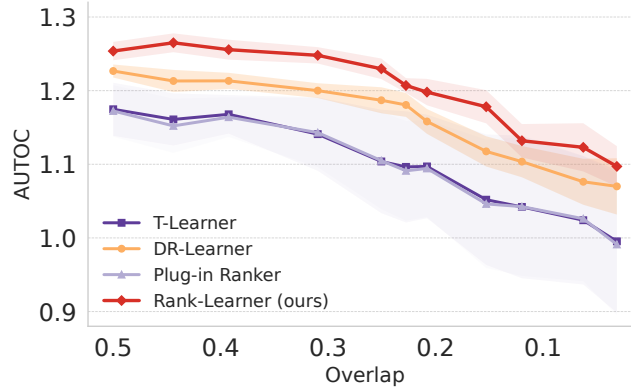


Figure 6. Synthetic benchmark (overlap sensitivity). Test AUTOOC (mean \pm s.e. over five seeds) as a function of overlap (decreasing left to right) for $n = 500$. *Higher is better*. Overlap is varied by changing treatment assignment, while the remaining components of the synthetic data-generating process are kept fixed.

F.3. Sensitivity to overlap

Figure 6 shows the effect of decreasing overlap on ranking performance across methods on the synthetic benchmark. In this experiment, we fix the training size to $n = 500$ and vary the overlap by modifying the treatment assignment mechanism, while keeping the remaining components of the synthetic data-generating process fixed (cf. Appendix E.1). Specifically, we have changed the propensity score to

$$e(X) = \sigma\left(\alpha(0.8s(X) + 0.6(X_6 - 0.5X_7))\right), \quad (135)$$

where larger values of α correspond to reduced overlap. The degree of overlap is then quantified as the empirical mean of $\min\{e(X), 1 - e(X)\}$ over the generated sample. We vary α such that this overlap measure ranges from approximately 0.5 (near random treatment assignment) to values below 0.05 (virtually no overlap). We observe qualitatively similar behavior for varying training sizes, and therefore report results for a representative sample size of $n = 500$. Across all methods, the ranking performance (measured by AUTOOC) degrades smoothly as overlap decreases. This also holds for the proposed *Rank-Learner*, but the method consistently achieves the strongest performance across the considered baselines.

F.4. Comparison to prior work on direct ranking of treatment effects

The main goal of our experimental design is to isolate the effect on ranking performance of (i) direct ranking versus standard CATE estimation and (ii) orthogonal versus plug-in objectives for ranking. Additionally, we compare *Rank-Learner* to the two recent papers that also study direct ranking of treatment effects (cf. Section 2). In particular, we include the tree-based approach of Kamran et al. (2024) as an additional baseline, which we denote *tree ranker*, and report results on the synthetic benchmark below. We do not include an additional baseline for Vanderschueren et al. (2024), since their empirical strategy

is already captured by our *plug-in ranker* in the main experiments (Table 5).

Both *Rank-Learner* and the *tree ranker* of Kamran et al. (2024) rely on nuisance functions. *Rank-Learner* uses estimated response surfaces and propensities in its orthogonal pairwise loss, while Kamran et al. (2024) construct doubly robust scores for their tree-based splitting criterion. To ensure a fair comparison, we use the *same* nuisance estimates for both methods, and only vary the second-stage ranking model. We further tune the hyperparameters of *tree ranker* using the same model selection protocol as for our models (cf. Appendix E.3): we search over tree depth $\in \{3, 4, 5\}$, number of trees $\in \{50, 100\}$, subsampling rate $\in \{0.4, 0.5, 0.6\}$, and leaf size $\in \{5, 10, 20, 30, 50\}$, and then fix the selected configuration across all seeds and training sizes.

Table 7. Synthetic benchmark (comparison to prior work): Test AUTOC and mean policy value (mean \pm std dev over five seeds) across training sizes. *Higher is better*. The oracle column reports the metrics obtained by ranking the test set using the true treatment effects. Best mean is shown in **bold**.

Metric	Method	$n = 100$	$n = 250$	$n = 500$	$n = 1,000$	$n = 2,000$	oracle
AUTOC (\uparrow)	Tree ranker	1.01 \pm 0.16	1.20 \pm 0.04	1.27 \pm 0.03	1.31 \pm 0.01	1.34 \pm 0.01	1.40
	Rank-learner (<i>ours</i>)	0.94 \pm 0.21	1.28 \pm 0.03	1.30 \pm 0.03	1.34 \pm 0.01	1.37 \pm 0.00	
\bar{V} (\uparrow)	Tree ranker	0.49 \pm 0.04	0.53 \pm 0.01	0.55 \pm 0.01	0.57 \pm 0.00	0.57 \pm 0.00	0.59
	Rank-learner (<i>ours</i>)	0.46 \pm 0.05	0.55 \pm 0.01	0.56 \pm 0.01	0.57 \pm 0.00	0.58 \pm 0.00	

Table 7 reports a comparison of *Rank-Learner* to the *tree ranker* of Kamran et al. (2024) on the synthetic benchmark. We find that *Rank-Learner* outperforms the method for training sizes $n \geq 250$ in terms of both AUTOC and mean policy value. Only at the smallest sample size ($n = 100$), *tree ranker* attains slightly higher AUTOC and mean policy value, although performance is also more variable at this sample size across methods. Overall, *Rank-Learner* consistently outperforms this model-specific baseline on the synthetic benchmark.

F.5. Results on the semi-synthetic benchmarks

Table 8 reports performance on the semi-synthetic datasets, where real-world covariates are combined with simulated treatments and outcomes. Across all considered datasets, the *Rank-Learner* achieves the strongest performance, outperforming the non-orthogonal plug-in ranker and the pointwise CATE estimators in terms of AUTOC and mean policy value. These results confirm that the advantages observed in the fully synthetic setting carry over to real-world feature distributions.

Table 8. Semi-synthetic benchmarks: Test AUTOC and mean policy value (mean \pm std dev over five seeds) with training size $n = 1,000$. *Higher is better*. The oracle column reports the metrics obtained by ranking the test set using the true treatment effects. Best mean is shown in **bold**.

Metric	Method	MOVIELENS	MIMIC-III	CPS
AUTOC (\uparrow)	T-learner	1.31 \pm 0.03	1.12 \pm 0.05	0.87 \pm 0.08
	DR-learner	1.34 \pm 0.02	1.16 \pm 0.02	0.92 \pm 0.02
	Plug-in ranker	1.30 \pm 0.03	1.11 \pm 0.05	0.87 \pm 0.08
	Rank-learner (<i>ours</i>)	1.35 \pm 0.01	1.18 \pm 0.02	0.95 \pm 0.01
	oracle	1.39	1.22	1.01
\bar{V} (\uparrow)	T-learner	0.78 \pm 0.01	0.95 \pm 0.02	1.43 \pm 0.03
	DR-learner	0.79 \pm 0.00	0.97 \pm 0.00	1.45 \pm 0.01
	Plug-in ranker	0.78 \pm 0.01	0.95 \pm 0.02	1.43 \pm 0.03
	Rank-learner (<i>ours</i>)	0.79 \pm 0.00	0.97 \pm 0.00	1.46 \pm 0.00
	oracle	0.80	0.98	1.48